Negative regulation of platelet function by a secreted cell repulsive protein, semaphorin 3A

Hirokazu Kashiwagi, Masamichi Shiraga, Hisashi Kato, Tsuyoshi Kamae, Naoko Yamamoto, Seiji Tadokoro, Yoshiyuki Kurata, Yoshiaki Tomiyama, and Yuzuru Kanakura

Semaphorin 3A (Sema3A) is a secreted disulfide-bound homodimeric molecule that induces growth cone collapse and repulsion of axon growth in the nervous system. Recently, it has been demonstrated that Sema3A is produced by endothelial cells and inhibits integrin function in an autocrine fashion. In this study, we investigated the effects of Sema3A on platelet function by using 2 distinct human Sema3A chimera proteins. We detected expression of functional Sema3A receptors in platelets and dose-dependent and saturable binding of Sema3A to platelets. Sema3A dose-dependently inhibited activation of integrin αIIbβ3 by all agonists examined including adenosine diphosphate (ADP), thrombin, convulxin, phorbol 12-myristate 13-acetate, and A23187. Sema3A inhibited not only platelet aggregation induced by thrombin or collagen but also platelet adhesion and spreading on immobilized fibrinogen. Moreover, Sema3A impaired αIIbβ3-independent spreading on glass coverslips and aggregation-independent granular secretion. Sema3A inhibited agonist-induced elevation of filamentous action (F-actin) contents, phosphorylation of cofilin, and Rac1 activation. In contrast, Sema3A did not affect the levels of cyclic nucleotides or agonist-induced increase of intracellular Ca^{2+} concentrations. Thus, the extensive inhibition of platelet function by Sema3A appears to be mediated, at least in part, through impairment of agonist-induced Rac1-dependent actin rearrangement. (Blood. 2005;106:913-921)

Introduction

Platelets play a crucial role not only in a hemostatic plug formation but also in a pathologic thrombus formation, particularly within atherosclerotic arteries subjected to high shear stress.[1,2] As an initial step in thrombogenesis, platelets adhere to altered vascular surfaces or exposed subendothelial extracellular matrices, then become activated and aggregate each other. These processes are primarily mediated by platelet surface glycoproteins such as GPIb-IX-V, integrin α2β1, GPVI, and integrin αIIbβ3.[3,4] Especially, integrin αIIbβ3 plays an essential part in aggregate formation and adhesive spreading of platelets during hemostasis.[5-7] Pathways that inhibit platelet function are as important as those that activate them. Endothelial cells produce 2 well-documented inhibitors of platelet activation and aggregation, prostaglandin I_2 (PGI_2) and nitric oxide (NO).[8] PGI_2 binds to a specific Gs-coupled receptor, thereby activating adenylate cyclase and cyclic adenosine monophosphate (cAMP)–dependent protein kinase or protein kinase A (PKA). NO activates soluble guanylate cyclase and cyclic guanosine monophosphate (cGMP)–dependent kinase or PKG. Ecto–adenosine diphosphatase (ADPase, CD39) located on the luminal surface of endothelial cells also inhibits platelet aggregation by decreasing the local concentration of ADP. Thus, endothelial dysfunction or damage promotes a prothrombotic state and may be involved in the pathogenesis of cardiovascular disorders, including atherosclerosis, diabetes mellitus, essential hypertension, hypercholesterolemia, and hyperhomocysteinemia.[8]

The semaphorin family comprises soluble and membrane-bound proteins that are defined by the presence of a conserved 500–amino acid semaphorin domain at their amino termini.[9] Class 3 semaphorins are secreted disulfide-bound homodimeric molecules, and Sema3A, a prototypic class 3 semaphorin, causes growth cone collapse and provides chemorepulsive guidance for migrating axons.[10-12] Cell surface receptor for Sema3A consists of a complex of 2 distinct transmembrane receptors, neuropilin-1 and plexin A (A1-A3).[10-13] Neuropilin-1 provides a binding site of Sema3A, while plexin A transduces the Sema3A signals into the cells through its cytoplasmic domain.[10-13] Although the intracellular signaling pathways evoked by Sema3A binding are not fully understood, plexins should interact with signaling molecules to regulate actin reorganization, since growth cone collapse is accompanied by rapid reorganization of the actin filaments normally present in lamellipodia or filopodia.[11,12] In this context, a Rho family small G-protein, Rac, has been identified as a potential regulator of semaphorin-dependent actin cytoskeletal dynamics.[11,12]

Although Sema3A function on neural development is studied intensively, its function in other organs is poorly understood. The fact that semaphorins are expressed in many different tissues suggests that they also play a role in systems other than

From the Department of Hematology and Oncology, Osaka University Graduate School of Medicine, Osaka, Japan; and the Department of Blood Transfusion, Osaka University Hospital, Osaka, Japan.

Submitted October 26, 2004; accepted April 10, 2005. Prepublished online as *Blood* First Edition Paper, April 14, 2005; DOI 10.1182/blood-2004-10-4092.

Supported in part by Grant-in-Aid for Scientific Research from the Ministry of Education, Science, and Culture in Japan; the Yamanouchi Foundation for Research and Metabolic Disorders, Tsukuba, Japan; and Mitsubishi Pharma Research Foundation, Osaka, Japan.

Reprints: Hirokazu Kashiwagi, Department of Hematology and Oncology, Osaka University Graduate School of Medicine, 2-2 Yamadaoka, Suita, Osaka 565-0871, Japan; e-mail: kashi@hp-blood.med.osaka-u.ac.jp.

The publication costs of this article were defrayed in part by page charge payment. Therefore, and solely to indicate this fact, this article is hereby marked "advertisement" in accordance with 18 U.S.C. section 1734.

the nervous system.[12] Indeed, in addition to neural abnormalities, mice lacking a functional *Sema3A* gene have abnormalities in their heart and visceral tissues, suggesting that Sema3A signaling might be indispensable for normal development in several organs.[14,15] Very recently, Serini et al reported that semaphorins are also involved in angiogenesis.[16] They showed that endothelial cells generate chemorepulsive autocrine signals of class 3 semaphorins that localize at nascent adhesive sites in spreading endothelial cells.[16] Interestingly, Sema3A inhibits the integrin-mediated adhesion to extracellular matrix and impedes their directional motility, which could explain the aberrant vascularization that is observed in Sema3A-deficient mice.[16] Others also showed that plexin signaling negatively regulates integrin-based adhesive complexes, which leads to the inhibition of cell adhesion, lamellipodia formation, and cell migration.[17]

Since integrin αIIbβ3 is essential for platelet function and endothelial cells express Sema3A, we sought to investigate the effects of Sema3A on platelet function. In this study, we demonstrate that Sema3A binds to platelets and inhibits αIIbβ3 activation extensively. Sema3A also inhibits platelet aggregate formation and platelet adhesion and spreading on immobilized fibrinogen. Moreover, Sema3A inhibits αIIbβ3-independent spreading on glass coverslips and aggregation-independent granular secretion. Further investigation of signaling pathways demonstrates that Sema3A markedly impairs agonist-induced Rac1-dependent actin rearrangement.

Materials and methods

Reagents

Recombinant human Sema3A fused to human Fc fragment (Sema3A/Fc) was obtained from R&D Systems (Minneapolis, MN). A construct consisting of the human *Sema3A* cDNA fused to the catalytic domain of human placental alkaline phosphatase (*AP*) cDNA was prepared as previously described using the pAP-tag2 expression vector (GenHunter, Nashville, TN).[10] The plasmid was transfected to 293T cells by Lipofectamine2000 (Invitrogen, Carlsbad, CA), and recombinant Sema3A/AP was purified from cultured medium using anti–human AP monoclonal antibody–conjugated sepharose beads (clone 8B6) and dialyzed against phosphate-buffered saline (PBS). Human IgG (hIgG) and human placental AP were used for controls of Sema3A/Fc and Sema3A/AP, respectively. Purity of Sema3A/Fc and Sema3A/AP was confirmed by 7.5% sodium dodecyl sulfate–polyacrylamide gel electrophoresis (SDS-PAGE) followed by silver staining (SilverSNAP Stain Kit; Pierce, Rockford, IL). Convulxin was kindly provided by Dr M. Moroi (Department of Protein Biochemistry, Institute of Life Science, Kurume University, Fukuoka, Japan). Fibrinogen was purchased from Calbiochem (San Diego, CA) and was labeled with fluorescein isothiocyanate (FITC), as previously described.[18] Type I collagen was obtained from MC Medical (Tokyo, Japan). A hybridoma producing IV.3, a mouse monoclonal antibody specific for human Fcγ-RIIA (CD32), was obtained from American Type Culture Collection (Rockville, MD) and IV.3 Fab fragments were generated as described previously.[19] All other reagents were purchased from Sigma (St Louis, MO), unless otherwise indicated.

Platelet preparation

Washed platelets were prepared as described previously.[20] In brief, 6 vol freshly drawn venous blood from healthy volunteers was mixed with 1 vol acid-citrate-dextrose and centrifuged at 250*g* for 10 minutes to obtain platelet-rich plasma (PRP). After a 5-minute incubation with 1 μM prostaglandin E_1 (PGE_1) and 1 U/mL apyrase, the PRP was centrifuged at 750*g* for 10 minutes, washed once with citrate buffer containing 1 μM PGE_1 and 1 U/mL apyrase, and resuspended in an appropriate buffer. Washed platelets were rested for 30 minutes at 37°C before use in any experiments. In all experiments using Sema3A/Fc, platelet FcγRIIA receptor was blocked by preincubation with 20 μg/mL IV.3 Fab.

Platelets for RNA extraction were prepared as described previously.[21] In brief, to remove the contaminated leukocytes, PRP was passed through a leukocyte removal filter (Sepacell PL-5A; Asahi Medical, Tokyo, Japan), which can remove more than 99.9% of contaminated leukocytes.[21]

Detection of binding of Sema3A to platelets and Sema3A receptors in platelets

For detection of binding of Sema3A/Fc to platelets, 5×10^5 washed platelets in Walsh buffer (137 mM NaCl, 2.7 mM KCl, 1.0 mM $MgCl_2$, 3.3 mM NaH_2PO_4, 3.8 mM HEPES [*N*-2-hydroxyethylpiperazine-*N*′-2-ethanesulfonic acid], 0.1% glucose, 0.1% bovine serum albumin [BSA], pH 7.4) were incubated with various concentrations of Sema3A/Fc for 30 minutes at room temperature and washed once with citrate buffer. Then, platelets were resuspended in PBS with FITC-labeled anti–human Fc for 20 minutes, followed by flow cytometric analysis. For detection of the binding of Sema3A/AP, 5×10^6 platelets were incubated with various concentrations of Sema3A/AP for 30 minutes at room temperature. After washing with citrate buffer, AP activity was measured using disodium phenylphosphate as a substrate (Sanko Jun-yaku, Tokyo, Japan). The number of Sema3A binding sites was estimated by the maximum AP activity of Sema3A/AP obtained from standard AP activity. In some experiments, platelets were first incubated with 125 μg/mL Sema3A/Fc or hIgG for 10 minutes. After washing, platelets were incubated with 10 μg/mL Sema3A/AP for another 30 minutes, and AP activity was measured.

Western blotting and flow cytometry of neuropilin-1 were performed with mouse anti–neuropilin-1 antibody (Santa Cruz Biotechnology, Santa Cruz, CA) as described previously.[22,23] Horseradish peroxidase (HRP)–conjugated anti–mouse IgG (New England Biolabs, Beverly, MA) and Alexa488-conjugated anti–mouse IgG (Molecular Probes, Eugene, OR) were used as secondary antibodies for Western blotting and flow cytometry, respectively. Reverse transcriptase–polymerase chain reaction (RT-PCR) for detection of plexin-A1, -A2, and -A3 was performed as described.[16] In brief, RNA was extracted by a Trizol reagent (Invitrogen), and cDNA was synthesized using Moloney murine leukemia virus (M-MLV) reverse transcriptase (Invitrogen). RT products were amplified in a PCR reaction with a Taq polymerase (Takara ExTaq; Takara Bio, Shiga, Japan). Primer sequences and PCR conditions were described previously.[16]

Activation of αIIbβ3 by various agonists

Activation state of αIIbβ3 was monitored by binding of a ligand-mimetic antibody, PAC-1, or soluble fibrinogen under flow cytometric analysis as described previously.[21,22,24] In brief, 5×10^5 platelets in Walsh buffer were preincubated with Sema3A/Fc or Sema3A/AP for 10 minutes, followed by incubation with agonists and FITC-conjugated PAC-1 (BD Biosciences, Franklin Lakes, NJ) or FITC-fibrinogen for 20 minutes at room temperature. Then, platelets were diluted to 500 μL with Walsh buffer and analyzed immediately on flow cytometry (FACScan; BD Japan, Tokyo, Japan).

Platelet aggregation study

Platelet aggregation was monitored using a platelet aggregometer (model 313M; MC Medical) at 37°C with a stirring rate at 1000 rpm, as previously described.[20] In brief, Sema3A/AP- or AP-treated platelets were suspended in modified Tyrode buffer containing 1 mM $MgCl_2$ at the concentration of $2 \times 10^5/\mu L$. After addition of $CaCl_2$ at the final concentration of 1 mM and incubation for one minute at 37°C, aggregation was initiated by addition of agonists.

Platelet granular secretion

Granular secretion was monitored by FITC-CD62P (Immunotech, Marseille, France) and phycoerythrin-conjugated CD63 (Immunotech) binding to platelets under flow cytometry as described previously.[25]

Adhesion to immobilized fibrinogen or glass coverslips

Adhesion of platelets to immobilized fibrinogen was assessed as described previously.[26] In brief, a 96-well polystyrene plate (Greiner Japan, Tokyo, Japan) was coated with fibrinogen at the various concentrations in PBS for 16 hours at 4°C. Platelets (1.25×10^6) in Tyrode buffer (137 mM NaCl, 12 mM $NaHCO_3$, 2.6 mM KCl, 1 mM $CaCl_2$, 1 mM $MgCl_2$, 5 mM HEPES, 0.1% glucose, 0.1% BSA, pH 7.4) were incubated with 20 μg/mL Sema3A/Fc or hIgG for 10 minutes at room temperature, and then they were placed on each well followed by incubation for one hour at room temperature. After washing 3 times with PBS to remove nonadherent platelets, adhered platelets were quantified by measuring endogenous cellular acid phosphate activity.[27] Relative adhesion to the maximum binding was calculated by dividing the acid phosphatase activity of adherent platelets by that of nontreated platelets adhered on the 10 μg/mL fibrinogen.

Morphologic study of adhered platelets was performed as described previously.[28] In brief, glass coverslips were coated with 20 μg/mL fibrinogen for 16 hours at 4°C, and then washed with PBS. After incubation with Sema3A/Fc or hIgG, 2×10^6 platelets in Tyrode buffer were incubated on the fibrinogen-coated coverslips for 45 minutes at 37°C or on the nontreated coverslips for 10 minutes at room temperature. Nonadherent platelets were washed away and adherent cells were stained with tetramethylrhodamine B isothiocyanate–conjugated phalloidin. Platelet spreading was observed under a florescence microscope (PROVIS AX-80; Olympus, Tokyo, Japan).

Quantification of F-actin contents

Filamentous actin (F-actin) content was analyzed by flow cytometry with bodipy-phallacidin as described previously.[28] In brief, after incubation with 20 μg/mL Sema3A/Fc or hIgG, platelets in Walsh buffer were stimulated with a 30-second incubation with 30 μM protease-activated receptor 1 (PAR1)–thrombin receptor-activating peptide (TRAP) or 0.5 U/mL thrombin at 37°C. Then, platelets were fixed with 4 vol of 2.6% glutaraldehyde in 5.3 mM EDTA (ethylenediaminetetraacetic acid) for 2 hours at 37°C. After washing twice with PBS, the platelets were resuspended to half their initial volume and incubated at 37°C either with 3.3 μM bodipy-phallacidin (Molecular Probes) or bodipy-phallacidin in the presence of a 300-fold molar excess of unlabeled phallacidin. After 30 minutes, the platelets were washed twice with PBS and platelet fluorescence was analyzed in the fluorescence intensity 1 (FL1) channel of the flow cytometer. Specific phallacidin binding was obtained by subtraction of mean fluorescence intensity of FL1 with unlabeled phallacidin from that of FL1 without unlabeled phallacidin.

Detection of phosphorylation of cofilin and activated Rac1

After incubation with 20 μg/mL Sema3A/Fc or hIgG for 10 minutes at room temperature, 1×10^7 platelets in Walsh buffer were incubated with 0.5 U/mL thrombin for the indicated times at 37°C without stirring. Then, cells were lysed with SDS sample buffer with 5% β-mercaptoethanol (β-ME). Proteins were resolved on a 15% SDS-PAGE gel and transferred to a polyvinylidene difluoride (PVDF) membrane (Immobilon-P; Millipore, Bedford, MA). Phosphorylated cofilin was detected by using anti–phospho-cofilin antibody (Cell Signaling Technology, Beverly, MA). After stripping the membrane with a stripping buffer (Restore Western Blot Stripping Buffer; Pierce), the membrane was rehybridzed with anticofilin antibody (BD Biosciences). Optical density of the bands was measured by National Institutes of Health (NIH) Image software (Bethesda, MD). After calibrating the density of phosphorylated cofilin with that of total cofilin, relative increase of phosphorylated cofilin against that of IgG-treated platelets without agonist stimulation was calculated.

Detection of activated Rac1 was performed using a kit of pull-down assay according to the manufacturer's directions (EZ-Detect Rac1 Activation Kit; Pierce). In brief, Sema3A/Fc- or hIgG-treated platelets in Walsh buffer were incubated with 30 μM PAR1-TRAP for the indicated times at 37°C without stirring. Then, cells were lysed with 0.5% Triton-X100 lysis buffer. Guanosine triphosphate (GTP)–form of Rac1 was pull-downed by incubation with glutathione-S–transferase (GST)–p21-activated kinase 1 (PAK1)–p21-binding domain (PBD) and glutathione beads for one hour at 4°C. After washing with lysis buffer, precipitates were eluted with SDS sample buffer with β-ME, followed by electrophoresis on a 12% SDS-PAGE gel. After transfer to a PVDF membrane, Rac1 was detected by a mouse anti-Rac1–specific antibody. Total Rac1 was detected by

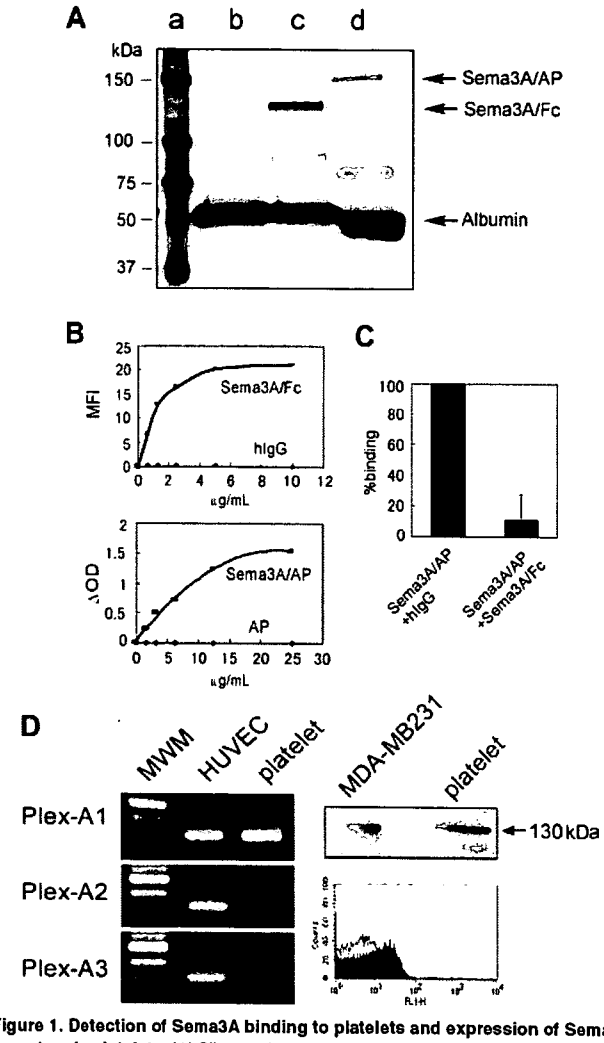

Figure 1. Detection of Sema3A binding to platelets and expression of Sema3A receptors in platelets. (A) Silver stain of purified Sema3A fusion proteins; 0.25 μg of Sema3A/Fc (~ 125 kDa, lane c) and Sema3A/AP (~ 150 kDa, lane d) were loaded on a 7.5% SDS-PAGE gel under reducing conditions and silver staining was performed. Sema3A/Fc and Sema3A/AP samples contain BSA as a carrier protein. In lane c, only BSA was loaded. Molecular weight marker was loaded in lane a. (B) Binding of Sema3A/Fc or Sema3A/AP to platelets. Washed platelets (5×10^5) were incubated with Sema3A/Fc or hIgG, followed by incubation with FITC anti–human Fc. Sema3A/Fc binding was detected by flow cytometry, and mean fluorescence intensity (MFI) was plotted in the top panel. Washed platelets (5×10^6) were incubated with Sema3A/AP or AP, and after washing, AP activity was measured using disodium phenylphosphate as a substrate. Change in optical density (ΔOD) was plotted on the bottom panel. Shown are representative results of 3 independent experiments. (C) Inhibition of Sema3A/AP binding by Sema3A/Fc. Washed platelets were first incubated with 125 μg/mL hIgG or Sema3A/Fc. Then, platelets were incubated with 10 μg/mL Sema3A/AP, and AP activity was measured. Shown is mean and SE of relative binding to hIgG-incubated sample of 3 independent experiments. (D) Expression of plexin-A1, -A2, or -A3 in platelets was detected by RT-PCR assay (left). Human umbilical vein endothelial cell (HUVEC) was used as a positive control. Expression of neuropilin-1 in platelets was detected by Western blotting and flow cytometric analysis (right). In Western blotting, neuropilin-1 expression was detected by anti–neuropilin-1 antibody, followed by incubation with HRP anti–mouse IgG. MDA-MB231 was used as a positive control. In flow cytometry, platelets were incubated with mouse monoclonal anti–neuropilin-1 antibody (filled curve) or control antibody (MOPC21; open curve), followed by incubation with Alexa488-conjugated anti–mouse IgG. MWM indicates molecular weight marker.

electrophoresis of total lysates on an SDS-PAGE gel followed by detection with the Rac1-specific antibody.

Intracellular Ca^{2+} mobilization

Intracellular Ca^{2+} concentrations in fluo-3–loaded platelets were assessed under flow cytometry as described previously.[29] In brief, platelets were labeled with 5 μM fluo-3-AM (Wako Pure Chemical, Osaka, Japan) at 37°C for 15 minutes. After incubation with 20 μg/mL Sema3A/Fc or hIgG, 5×10^5 platelets in 200 μL Walsh buffer were subjected to flow cytometry analysis. After the determination for about 10 seconds of baseline fluo-3 fluorescence from the platelet population, cell aspiration into the flow cytometry was briefly paused, and 1:10 volume of 5 U/mL thrombin was added. The acquisition was then resumed, and changes in log fluorescence versus time were recorded. For each plot, rectangular analysis regions were defined over the time axis, and mean florescence intensity was calculated with CellQuest software (BD Japan).

Quantification of platelet cyclic nucleotide levels

For cAMP quantification, 1.6×10^6 platelets in Walsh buffer were incubated with 20 μg/mL Sema3A/Fc or hIgG for 10 minutes at room temperature. Iloprost (20 μg/L; Cayman Chemical, Ann Arbor, MI) was used as an agonist for activation of adenylate cyclase. ADP (5 μM) was added to the platelet samples and incubated for 2 minutes at room temperature to study inhibition of adenylate cyclase. After lysing platelets, cAMP contents were measured by an enzyme immunoassay kit according to the manufacturer's directions (Biotrak cAMP EIA System; Amersham, Piscataway, NJ). For cGMP quantification, 3.6×10^6 platelets in Walsh buffer were incubated with 20 μg/mL Sema3A/Fc or hIgG for 10 minutes at room temperature, and cGMP contents were measured by an EIA kit (Biotrak cGMP EIA System; Amersham).

Statistical analysis

Experimental differences over the controls were analyzed by the Student *t* test. Probability values of *P* less than .05 were considered significant.

Results

Binding of Sema3A to platelets and expression of Sema3A receptors in platelets

We used 2 distinct Sema3A chimera proteins in this study: recombinant human Sema3A fused to human Fc fragment (Sema3A/Fc) or to the catalytic domain of human placental alkaline phosphatase (Sema3A/AP) (Figure 1A). We first investigated the binding of Sema3A to platelets. As shown in Figure 1B (upper), Sema3A/Fc bound to platelets in a dose-dependent and saturable manner. Sema3A/AP also bound to the platelets in basically the same manner as Sema3A/Fc, although it needed about 2-fold concentrations, compared with Sema3A/Fc, to saturate the binding to platelets (Figure 1B lower). About 90% of the Sema3A/AP binding was inhibited by preincubation with excess amounts of Sema3A/Fc, confirming the specificity of Sema3A binding to platelets (Figure 1C). We estimated the binding sites of Sema3A were approximately 8000 (7980 ± 500, n = 4) per platelet.

Next, we examined expression of Sema3A receptors in platelets. Western blotting and flow cytometric analysis revealed that neuropilin-1 was expressed in platelets (Figure 1C). Plexin expression was examined by RT-PCR assay, using platelet samples in which the contaminated leukocytes were removed by a leukocyte removal filter. As shown in Figure 1C, plexin-A1 and low levels of plexin-A2 and plexin-A3 were expressed in platelets. These results suggest that platelets express functional Sema3A receptors.

Effects of Sema3A on αIIbβ3 activation by various agonists and platelet aggregation

Since Sema3A inhibits integrin function in endothelial cells,[16] we examined the effects of Sema3A on integrin αIIbβ3 activation using a ligand-mimetic antibody, PAC-1. Sema3A/Fc dose-dependently inhibited PAC-1 binding induced by all agonists examined, including agonists that act via G-protein–coupled receptors (ie, ADP, thrombin, and U46619) and convulxin, which acts via G-protein–uncoupled receptor, GPVI (Figure 2A; Table 1). Sema3A/Fc inhibited A23187- and phorbol 12-myristate 13-acetate (PMA)–induced PAC-1 binding, suggesting that Sema3A inhibits αIIbβ3 activation mainly downstream of intracellular calcium mobilization and protein kinase C activation. Sema3A/AP also inhibited αIIbβ3 activation by thrombin and ADP (Figure 2B), indicating that the inhibitory effects were caused by the Sema3A domain, not by the fused Fc or AP domain. Sema3A/Fc inhibited a physiologic ligand, soluble fibrinogen binding to platelets after

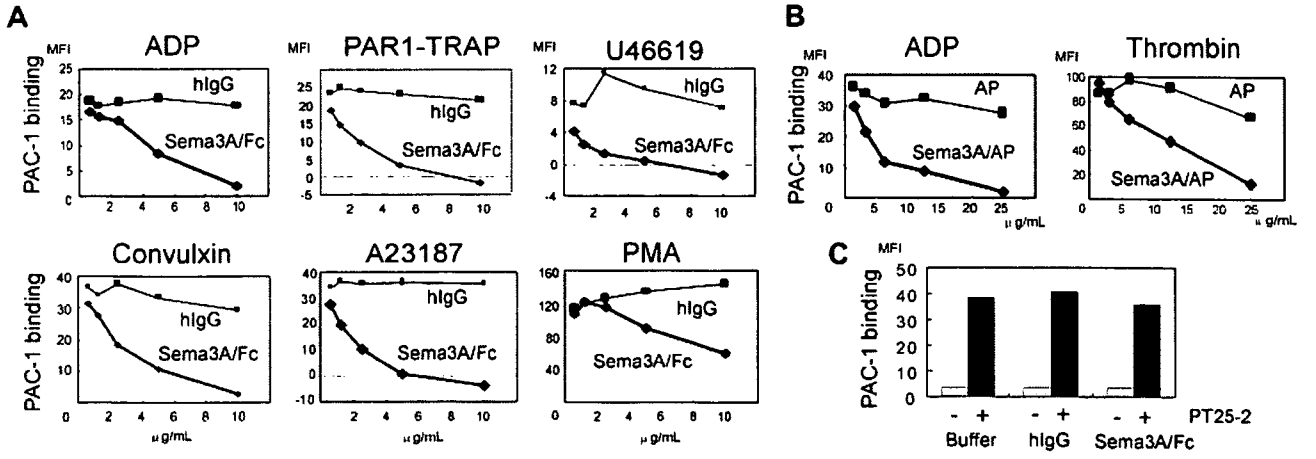

Figure 2. Inhibition of αIIbβ3 activation by Sema3A. (A) Washed platelets preincubated with the indicated concentrations of Sema3A/Fc (◆ and bold lines) or hIgG (■ and thin lines) were activated with ADP (5 μM), PAR1-TRAP (15 μM), U46619 (2 μM), convulxin (5 ng/mL), A23187 (2.5 μM), or PMA (200 nM). Activated αIIbβ3 was detected by binding of FITC–PAC-1. Shown are representative results of 3 to 5 independent experiments. (B) Washed platelets were preincubated with Sema3A/AP (◆ and bold lines) or AP (■ and thin lines) and activated by ADP (5 μM) or thrombin (0.5 U/mL), and then FITC–PAC-1 binding was detected. Shown are representative results of 3 independent experiments. (C) PBS-, hIgG-, or Sema3A/Fc-treated platelets were incubated with or without an αIIbβ3-activating antibody, PT25-2, and PAC1 binding was examined. Shown are representative results of 3 independent experiments.

Table 1. Inhibition of agonist-induced PAC1 binding by Sema3A

Agonist	Concentration (% inhibition)
ADP, μM	5 (90.4 ± 12.1)
PAR1-TRAP, μM	15 (115.2 ± 10.2)
Thrombin, U/mL	0.5 (97.4 ± 3.3)
U46619, μM	2 (112.5 ± 9.3)
Convulxin, ng/mL	5 (94.7 ± 6.0)
A23187, μM	2.5 (106 ± 5.5)
PMA, nM	200 (58.1 ± 14.3)

Platelets preincubated with 10 μg/mL Sema3A/Fc were activated with indicated agonists, and FITC-PAC1 binding was detected as demonstrated in Figure 2. Percent inhibition of mean fluorescent intensity against hIgG-treated platelets was calculated. Data represent mean ± SE of at least 3 independent experiments.

ADP and PAR1-TRAP stimulation, as well as PAC-1 binding (data not shown). PAC-1 binding with PT25-2, an anti-αIIbβ3 antibody that induces activated conformation of αIIbβ3 without intracellular signaling, was unaffected by preincubation with Sema3A (Figure 2C), indicating that Sema3A does not disturb PAC-1 binding competitively to its receptor. Since activation of αIIbβ3 leads to ligand binding and platelet aggregate formation, we studied the effects of Sema3A on platelet aggregation. Sema3A/AP impaired aggregate formation in low concentrations of collagen and thrombin (Figure 3), although it was hard to detect the inhibitory effects of Sema3A on platelet aggregation in high concentrations of the agonists.

Effects of Sema3A on granular secretion

We examined effects of Sema3A binding to platelets on granular secretion after ADP and thrombin stimulation. Surface expression of CD62P and CD63 was used for monitoring the secretion of alpha granule and dense or lysosome granule, respectively.[30] Sema3A/Fc dose-dependently inhibited surface expression of both CD62P and CD63 after ADP and thrombin stimulation without stirring, indicating that Sema3A inhibits aggregation-independent granule secretion induced by platelet agonists (Figure 4).

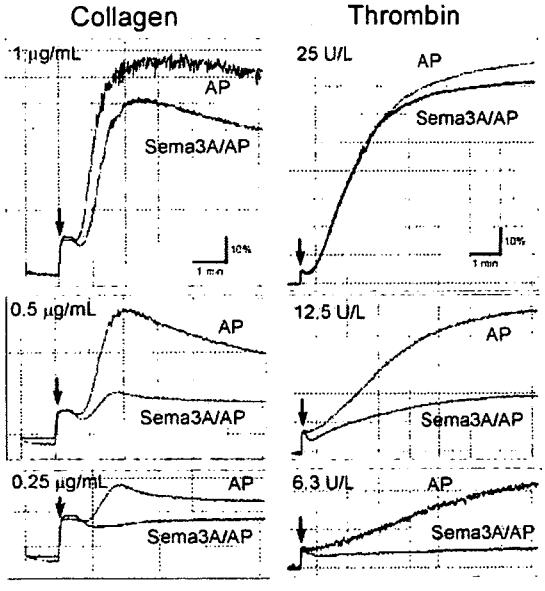

Figure 3. Inhibition of platelet aggregation by Sema3A. Washed platelets preincubated with 20 μg/mL Sema3A/AP or AP were activated with the indicated concentrations of collagen (left column) or thrombin (right column). Platelet aggregation was monitored using a platelet aggregometer. Arrow indicates the addition of agonists. Shown are representative results of 3 independent experiments.

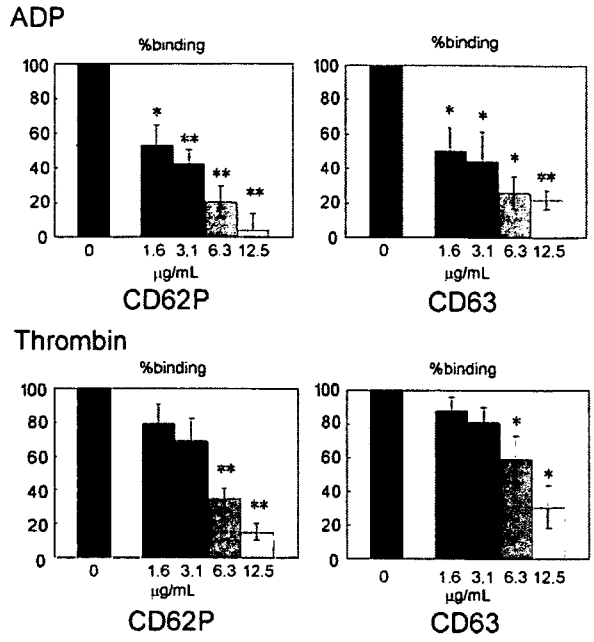

Figure 4. Inhibition of agonist-induced granular secretion by Sema3A. Washed platelets were preincubated with the indicated concentrations Sema3A/Fc, and then activated with ADP (5 μM) or thrombin (0.5 U/mL). Granular secretion was assessed by FITC-CD62P and PE-CD63 binding to platelets, and percent binding against hIgG-treated platelets was calculated. Shown are mean ± SE of percent binding of 3 independent experiments. $^{*}P < .05$; $^{**}P < .01$.

Effects of Sema3A on platelet adhesion and spreading

We next examined the effects of Sema3A on platelet adhesion to immobilized fibrinogen or nonspecific glass coverslips under static conditions. Quantification of adhered platelets by acid phosphatase method showed that preincubation with 20 μg/mL Sema3A/Fc led to about 20% reduction in platelet adhesion at every concentration of fibrinogen examined (Figure 5A). Microscopic examination demonstrated that after 45 minutes of incubation on 20 μg/mL fibrinogen, more than 80% of platelets showed full spreading (Figure 5Bi). In sharp contrast, spreading of Sema3A-treated platelets was markedly impaired (Figure 5Bii). The inhibition of platelet spreading by Sema3A was not αIIbβ3 specific, since Sema3A also inhibited platelet spreading on noncoated glass coverslips (Figure 5Biii-iv).

Effects of Sema3A on agonist-induced cytoskeleton rearrangement of platelets

The remarkable inhibition of platelet spreading by Sema3A suggests that Sema3A affects cytoskeletal rearrangement of platelets. To address the hypothesis, we quantified F-actin contents in platelets using bodipy-phallacidin and flow cytometry. Thrombin and PAR1-TRAP induced elevation of F-actin as demonstrated,[28] and Sema3A significantly impaired the elevation of agonist-induced F-actin elevation (Figure 6A). Cofilin is a protein that promotes severing and depolymerization of F-actin,[31,32] and involvement of cofilin in Sema3A signaling has been demonstrated.[31] Therefore, we next examined phosphorylation of cofilin after PAR1-TRAP stimulation. Sema3A decreased the level of phosphorylated cofilin in both resting and PAR1-TRAP–stimulated platelets, suggesting that Sema3A may keep cofilin in the dephosphorylated, activated state and increase severing of F-actin (Figure 6B). Since phosphorylation of cofilin is regulated by LIM kinase,[31,32] an effecter of Rac-PAK signaling pathway,[33] and the involvement of

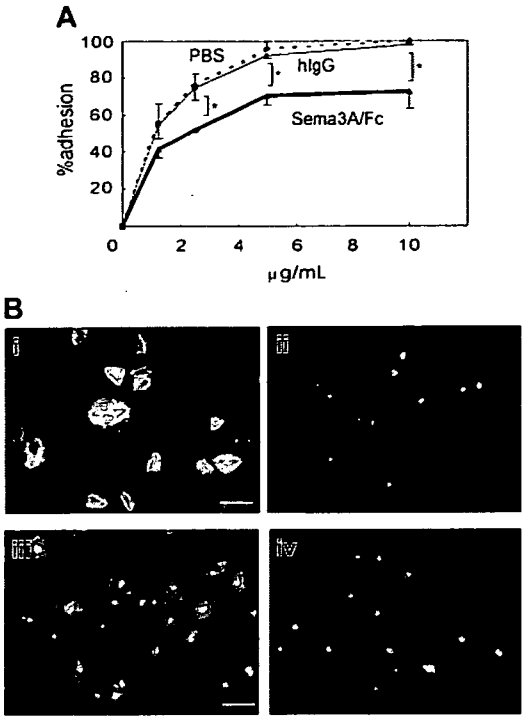

Figure 5. Effects of Sema3A on platelet adhesion and spreading. (A) Washed platelets were incubated with 20 μg/mL Sema3A/Fc (bold line) or hIgG (thin solid line), or PBS (dashed line), and then placed on the various concentrations of immobilized fibrinogen for one hour. After washing with PBS to remove nonadherent platelets, adhered platelets were quantified by acid phosphatase method. Mean and SE of percent adhesion of 3 independent experiments was plotted. $^*P < .05$. (B) Sema3A-treated platelets (ii,iv) or hIgG-treated platelets (i,iii) were placed on fibrinogen-coated (i-ii) or nontreated (iii-iv) glass coverslips. Adhered platelets were stained with TRICT (tetramethylrhodamine-5(and 6)-isothiocyanate)–phalloidin. Images were captured with a CCD camera (DP-70; Olympus) mounted on an Olympus AX-80 fluorescence microscope equipped with a 100 ×/1.30 oil immersion objective lens. Images were acquired with Olympus DP Controller software and processed with Adobe Photoshop Elements 2.0 (Adobe Systems, San Jose, CA). Original magnification × 1000, and bar in panel Bi represents 10 μm.

Rac in semaphorin signaling is well demonstrated,[11,12] we examined the effects of Sema3A on Rac1 activation by PAR1-TRAP. Consistent with previous reports,[34,35] PAR1-TRAP induced rapid activation of Rac1 in platelets at the maximum in 30 seconds, and Sema3A almost completely inhibited the Rac1 activation induced by PAR1-TRAP (Figure 6C). These results suggest that Sema3A inhibits agonist-induced actin rearrangement via Rac1-dependent pathway including phosphorylation of cofilin.

Some reports demonstrated that Sema3A affects another cytoskeletal component, microtubule rearrangement.[36,37] However, we did not observe any apparent effects of Sema3A on tubulin staining in platelets (data not shown).

Effects of Sema3A on Ca^{2+} and cyclic nucleotide signaling in platelets

To examine whether Sema3A may affect Ca^{2+} signaling, fluo-3–loaded platelets were stimulated with thrombin and intracellular Ca^{2+} concentrations were monitored under flow cytometry. Thrombin induced rapid increase in intracellular Ca^{2+} concentrations in control platelets as described,[20] and Sema3A/Fc did not affect the thrombin-induced increase in intracellular Ca^{2+} concentrations (Figure 7).

Since the best characterized platelet inhibitory signaling pathways are cyclic nucleotide pathways,[38] we finally examined the effects of Sema3A on cyclic nucleotides in platelets. Sema3A did not increase the basal cAMP level in nonstimulated platelets per se (Table 2). Stable prostacyclin, iloprost, elevates intracellular cAMP, and addition of ADP impairs the iloprost-induced cAMP elevation by inhibiting adenylate cyclase.[39] Again, Sema3A treatment did not change cAMP contents in iloprost- and ADP-treated platelets (Table 2). Sema3A also had no effects on basal cGMP contents, whereas sodium nitroprusside, a stimulator of NO/protein kinase G pathway, induced elevation of cGMP contents (Table 3). Moreover, a nitric oxide synthase (NOS) inhibitor, L-nitroarginine methyl ester, or a NO-donor, L-arginine, had no effects on the inhibition of αIIbβ3 activation by Sema3A (data not shown).[40] These results suggest that neither cAMP nor cGMP is involved in inhibition of platelet function by Sema3A.

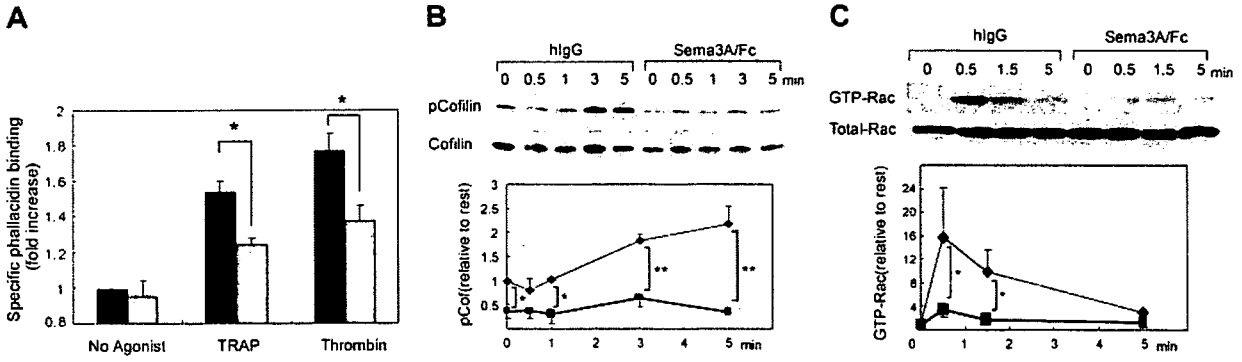

Figure 6. Effects of Sema3A on F-actin contents, cofilin phosphorylation, and Rac1 activation. (A) Sema3A/Fc- (gray bars) or hIgG-treated (black bars) platelets were activated by 30 μM PAR1-TRAP or 0.5 U/mL thrombin at 37°C for 30 seconds without stirring. After fixation, F-actin was stained with bodipy-phallacidin. Specific phallacidin binding was obtained by subtraction of FL1 fluorescence with a 300-fold more excess of unlabeled phallacidin from FL1 fluorescence without unlabeled phallacidin, and fold increase against fluorescence of no agonist sample was calculated. Data represent mean and SE of 3 independent experiments. $^*P < .05$. (B) Sema3A/Fc- or hIgG-treated platelets were activated with 30 μM PAR1-TRAP for the indicated time at 37°C without stirring. Then, cells were lysed and SDS-PAGE was performed. Phospho-cofilin was detected by anti–phospho-cofilin–specific antibody. After stripping, total cofilin was detected by anticofilin antibody. Optical density of the bands was measured by NIH Image software, and relative increase against phospho-cofilin in IgG-treated platelets without thrombin was calculated. Mean and SE of 3 independent experiments was plotted in bottom panel. $^*P < .05$; $^{**}P < .01$. (C) Sema3A/Fc- or hIgG-treated platelets were activated with 30 μM PAR1-TRAP for the indicated time at 37°C without stirring. GTP-form of Rac1 was precipitated by incubation with GST-PAK1-PBD and glutathione beads. After SDS-PAGE electrophoresis, Rac1 was detected by a Rac1-specific antibody. Total Rac was detected by electrophoresis of total lysates on an SDS-PAGE gel followed by detection with the same antibody. Optical density of the bands was measured by NIH Image software, and relative increase against GTP-Rac in IgG-treated platelets without thrombin was calculated. Sema3A/Fc is indicated by ■ and bold lines; hIgG, by ◆ and thin lines. Mean and SE of 3 independent experiments was plotted in lower panel. $^*P < .05$.

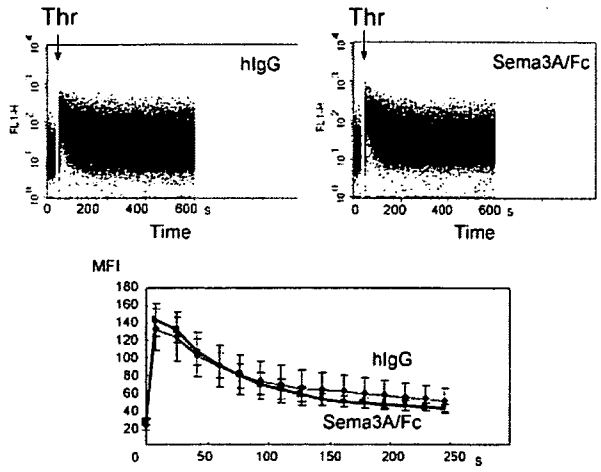

Figure 7. Effects of Sema3A on thrombin-induced increase of intracellular Ca^{2+} concentrations. Fluo-3–labeled platelets were incubated with 20 μg/mL Sema3A/Fc or hIgG. After the determination for about 10 seconds of baseline fluo-3 fluorescence from the platelet population, cell aspiration into the flow cytometry was briefly paused, and 1:10 volume of 5 U/mL thrombin (Thr) was added. The acquisition was then resumed, and changes in log fluorescence versus time were recorded (top panels). For each plot, rectangular analysis regions were defined over the time axis, and mean fluorescence intensity was calculated. Mean ± SE of 3 independent experiments was plotted in bottom panel. Bold and thin lines represent Sema3A/Fc and hIgG, respectively.

Discussion

In this report, we demonstrated for the first time the binding of Sema3A on platelets and extensive inhibitory effects of Sema3A on platelet function. As reported in endothelial cells,[16] Sema3A inhibited integrin-mediated function in platelets (ie, inhibition of αIIbβ3 activation and platelet aggregate formation, and adhesion and spreading on immobilized fibrinogen). However, Sema3A also inhibited αIIbβ3-independent adhesion and spreading on non-treated glass coverslips and aggregation-independent granular secretion. Although the most potent platelet inhibitory pathways are cyclic nucleotide pathways,[38] we did not detect any effect on cAMP and cGMP contents by Sema3A treatment. Thrombin-induced Ca^{2+} signaling was also unaffected by Sema3A treatment.

Sema3A markedly impaired αIIbβ3-independent as well as αIIbβ3-dependent platelet spreading. We demonstrated that Sema3A inhibited the increase of F-actin contents after thrombin or PAR1-TRAP stimulation. Thus, Sema3A inhibited adhesion-induced and agonist-induced actin rearrangement. Furthermore, Sema3A inhibited phosphorylation of cofilin and Rac1 activation after PAR1-TRAP stimulation. Several reports revealed that Rac1 activation is necessary for platelet actin assembly and lamellipodia formation after agonist stimulation.[34,35,41] Therefore, marked impairment of Rac1 activation is very likely to account for the Sema3A-induced impairment of actin rearrangement and spreading in platelets. There were 2 major downstream effectors of Rac1 identified, PAK and WAVEs ([Wiskott-Aldrich syndrome protein] WASP family Verprolin-homologous proteins).[42] Several PAK substrates or binding partners have been implicated in the effects of PAK, including filamin, LIM kinase, myosin, and paxillin.[43] Among them, LIM kinase phosphorylates and inactivates cofilin, a protein that promotes severing and depolymerization of F-actin.[31,32] Consistent with the inhibition of Rac1 activation, Sema3A inhibited phosphorylation of cofilin in both resting and activated platelets, suggesting that Sema3A increases severing and depolymerization of F-actin by keeping cofilin in the activated state. Rac1 inhibition by Sema3A might affect the activation of another major downstream effector of Rac1, WAVEs. WAVEs, also known as Scar, belong to the WASP family and activate actin-related protein 2 and 3 (Arp2/3) complex, resulting in nucleating actin polymerization.[43] Others and we have demonstrated that platelets contain WAVE isoforms and may regulate lamellipodia formation.[44,45] Therefore, it is also likely that Sema3A may inhibit actin rearrangement via inhibition of WAVE-dependent initiation of actin polymerization.

Table 2. Effects of Sema3A on cAMP

	cAMP, pmol/10^8 platelets
hIgG, 20 μg/mL	1.06 ± 0.19*
Sema3A/Fc, 20 μg/mL	1.00 ± 0.68*
Iloprost, 20 μg/L	45.94 ± 5.31
Iloprost, 20 μg/L + ADP, 5 μM + hIgG, 20 μg/mL	7.34 ± 0.47†
Iloprost, 20 μg/L + ADP, 5 μM + Sema3A/Fc, 20 μg/mL	5.66 ± 0.90†

Data represent the mean ± SE of 3 independent experiments.
*$P = .94$.
†$P = .24$.

Table 3. Effects of Sema3A on cGMP

	cGMP, pmol/10^8 platelets
hIgG, 20 μg/mL	0.83 ± 0.08*
Sema3A/Fc, 20 μg/mL	0.86 ± 0.04*
Sodium nitroprusside, 1 mM	5.56 ± 0.83

Data represent the mean ± SE of 3 independent experiments.
*$P = .70$.

In contrast to our results, it has been demonstrated that Rac1 activation is essential for Sema3A-induced growth cone collapse in neural cells,[46,47] and Sema3A-induced phosphorylation of cofilin is necessary for the process.[48] However, in these reports, the authors analyzed direct signaling induced by the binding of Sema3A. In this study, we analyzed the effects of Sema3A binding on agonist-induced signaling in platelets. Interestingly, Aizawa et al also found that phosphorylated cofilin was subsequently dephosphorylated within 5 minutes at the neural growth cone and the phosphorylated level of cofilin decreased to 0.16-fold of that of untreated growth cone,[48] which is consistent with our observation that cofilin is dephosphorylated in Sema3A-treated platelets. Signaling pathways from semaphorin receptors to Rac have not been fully understood even in neural cells.[11,12] Human plexin-B1, a receptor for Sema4D, and fly plexin B interact with activated Rac directly, and it has been suggested that these plexins sequester activated Rac and antagonize its signaling pathway.[49-51] Very recently Turner et al reported the association of activated Rac and the cytoplasmic tail of plexin-A1,[52] although others failed to detect the interaction.[50,53] Further studies are necessary to reveal the mechanism of regulation of Rac by Sema3A in platelets.

Is the impairment of actin rearrangement via inhibition of Rac1 responsible for Sema3A-induced extensive negative regulation of platelet function other than platelet spreading? To investigate the role of actin rearrangement on platelet function, effects of cytochalasins or latrunculin A, inhibitors of actin polymerization, have been studied.[54-58] There are some discrepancies in these reports, mainly because of the differences in experimental conditions; some reports demonstrated that high concentrations of cytochalasins inhibited agonist-induced αIIbβ3 activation and platelet aggregation, indicating that de novo actin polymerization affects activation of αIIbβ3,[54,55,58] whereas low concentrations of cytochalasin D and latrunculin A activated αIIbβ3.[57] Integrin activating inside-out

signaling consists of 2 aspects: conformational change that regulates integrin affinity and integrin clustering that regulates its avidity.[5,7] αIIbβ3 clustering may be promoted by actin cytoskeletal rearrangement, although conformational change seems to be the dominant way in αIIbβ3 activation.[59] Moreover, recent reports revealed that talin binding to integrin cytoplasmic tails is essential for integrin activation.[60,61] Since talin links integrin to actin filaments in clustering of integrins into adhesion complexes,[62,63] defects of actin polymerization may impair broad aspects of integrin signaling. However, impairment of actin rearrangement does not appear to be the sole mechanism of Sema3A inhibition of platelet function, since, in contrast to Sema3A, cytochalasins have no inhibitory effects on granular secretion.[55,58] Rac1 regulates many cellular activities besides cytoskeletal rearrangement, such as cell polarity and vesicle trafficking in other cells.[42] Moreover, Sema3A may act via Rac1-independent pathways (eg, the collapsin response mediator protein (CRMP)–mediated pathway).[12] These hypotheses remain to be determined.

It has been well documented that endothelial cells negatively regulate platelet function by secreted PGI_2, NO, and membrane-bound ecto-ADPase.[8] Since Sema3A is also produced in endothelial cells and inhibits platelet function extensively, Sema3A may contribute to maintain blood flow in normal, injured, or newly synthesized vessels by keeping platelets in the resting state. Moreover, since Sema3A appears to inhibit platelet function via unique Rac1-dependent pathway, modulation of Sema3A-inducing signaling pathway may be a new target of antiplatelet therapy.

In conclusion, we demonstrated that Sema3A binds to platelets and inhibits platelet function extensively. The inhibition of platelet function by Sema3A appeared to be mediated, at least in part, through impairment of agonist-induced Rac1-dependent actin rearrangement. We believe that these results reveal a new Sema3A function on thrombosis and hemostasis, and a unique inhibitory signaling pathway evoked by Sema3A binding to platelets.

Acknowledgment

We are grateful to Dr M. Moroi (Department of Protein Biochemistry, Institute of Life Science, Kurume University, Fukuoka, Japan) for providing us with convulxin.

References

1. Fuster V, Badimon L, Badimon JJ, Chesebro JH. The pathogenesis of coronary artery disease and the acute coronary syndromes. N Engl J Med. 1992;326:242-250.
2. Antithrombotic Trialists' Collaboration. Collaborative meta-analysis of randomised trials of antiplatelet therapy for prevention of death, myocardial infarction, and stroke in high risk patients. BMJ. 2002;324:71-86.
3. Savage B, Almus-Jacobs F, Ruggeri ZM. Specific synergy of multiple substrate-receptor interactions in platelet thrombus formation under flow. Cell. 1998;94:657-666.
4. Tomiyama Y, Shiraga M, Shattil SJ. Platelet membrane proteins as adhesion receptors. In: Gresele P, Page C, Fuster V, Vermylem J, eds. Platelets in Thrombotic and Non-Thrombotic Disorders. Cambridge, United Kingdom: Cambridge University Press; 2002:80-92.
5. Shattil SJ, Kashiwagi H, Pampori N. Integrin signaling: the platelet paradigm. Blood. 1998;91:2645-2657.
6. Tomiyama Y. Glanzmann thrombasthenia: integrin αIIbβ3 deficiency. Int J Hematol. 2000;72:448-454.
7. Shattil SJ, Newman PJ. Integrins: dynamic scaffolds for adhesion and signaling in platelets. Blood. 2004;104:1606-1615.
8. Pearson JD. Endothelial cell function and thrombosis. Baillieres Best Pract Res Clin Haematol. 1999;12:329-341.
9. Pasterkamp RJ, Kolodkin AL. Semaphorin junction: making tracks toward neural connectivity. Curr Opin Neurobiol. 2003;13:79-89.
10. Kolodkin AL, Levengood DV, Rowe EG, Tai YT, Giger RJ, Ginty DD. Neuropilin is a semaphorin III receptor. Cell. 1997;90:753-762.
11. Tamagnone L, Comoglio PM. Signalling by semaphorin receptors: cell guidance and beyond. Trends Cell Biol. 2000;10:377-383.
12. Goshima Y, Ito T, Sasaki Y, Nakamura F. Semaphorins as signals for cell repulsion and invasion. J Clin Invest. 2002;109:993-998.
13. Antipenko A, Himanen JP, van Leyen K, et al. Structure of the semaphorin-3A receptor binding module. Neuron. 2003;39:589-598.
14. Behar O, Golden JA, Mashimo H, Schoen FJ, Fishman MC. Semaphorin III is needed for normal patterning and growth of nerves, bones and heart. Nature. 1996;383:525-528.
15. Taniguchi M, Yuasa S, Fujisawa H, et al. Disruption of semaphorin III/D gene causes severe abnormality in peripheral nerve projection. Neuron. 1997;19:519-530.
16. Serini G, Valdembri D, Zanivan S, et al. Class 3 semaphorins control vascular morphogenesis by inhibiting integrin function. Nature. 2003;424:391-397.
17. Barberis D, Artigiani S, Casazza A, et al. Plexin signaling hampers integrin-based adhesion, leading to Rho-kinase independent cell rounding, and inhibiting lamellipodia extension and cell motility. FASEB J. 2004;18:592-594.
18. Honda S, Tomiyama Y, Aoki T, et al. Association between ligand-induced conformational changes of integrin $\alpha_{IIb}\beta_3$ and $\alpha_{IIb}\beta_3$-mediated intracellular Ca^{2+} signaling. Blood. 1998;92:3675-3683.
19. Tomiyama Y, Tsubakio T, Piotrowicz RS, Kurata Y, Loftus JC, Kunicki TJ. The Arg-Gly-Asp (RGD) recognition site of platelet glycoprotein IIb-IIIa on nonactivated platelets is accessible to high-affinity macromolecules. Blood. 1992;79:2303-2312.
20. Shiraga M, Tomiyama Y, Honda S, et al. Involvement of Na^+/Ca^{2+} exchanger in inside-out signaling through the platelet integrin $\alpha_{IIb}\beta_3$. Blood. 1998;92:3710-3720.
21. Kashiwagi H, Honda S, Tomiyama Y, et al. A novel polymorphism in glycoprotein IV (replacement of proline-90 by serine) predominates in subjects with platelet GPIV deficiency. Thromb Haemost. 1993;69:481-484.
22. Kashiwagi H, Tomiyama Y, Tadokoro S, et al. A mutation in the extracellular cysteine-rich repeat region of the β_3 subunit activates integrins $\alpha_{IIb}\beta_3$ and $\alpha_v\beta_3$. Blood. 1999;93:2559-2568.
23. Kashiwagi H, Shiraga M, Honda S, et al. Activation of integrin $\alpha_{IIb}\beta_3$ in the glycoprotein Ib-high population of a megakaryocytic cell line, CMK, by inside-out signaling. J Thromb Haemost. 2004;2:177-186.
24. Kashiwagi H, Schwartz MA, Eigenthaler M, Davis KA, Ginsberg MH, Shattil SJ. Affinity modulation of platelet integrin $\alpha_{IIb}\beta_3$ by β_3-endonexin, a selective binding partner of the β_3 integrin cytoplasmic tail. J Cell Biol. 1997;137:1433-1443.
25. Hayashi S, Oshida M, Kiyokawa T, et al. Determination of activated platelets: evaluation of methodology and application for patients with idiopathic thrombocytopenic purpura. Rinsho Byori. 2001;49:1287-1292.
26. Kiyoi T, Tomiyama Y, Honda S, et al. A naturally occurring Tyr143Hisα_{IIb} mutation abolishes $\alpha_{IIb}\beta_3$ function for soluble ligands but retains its ability for mediating cell adhesion and clot retraction: comparison with other mutations causing ligand-binding defects. Blood. 2003;101:3485-3491.
27. Bellavite P, Andrioli G, Guzzo P, et al. A colorimetric method for the measurement of platelet adhesion in microtiter plates. Anal Biochem. 1994;216:444-450.
28. Leng L, Kashiwagi H, Ren XD, Shattil SJ. RhoA and the function of platelet integrin $\alpha_{IIb}\beta_3$. Blood. 1998;91:4206-4215.
29. do Ceu Monteiro M, Sansonetty F, Goncalves MJ, O'Connor JE. Flow cytometric kinetic assay of calcium mobilization in whole blood platelets using Fluo-3 and CD41. Cytometry. 1999;35:302-310.
30. Rendu F, Brohard-Bohn B. Platelet organelles. In: Gresele P, Page C, Fuster V, Vermylem J, eds. Platelets in Thrombotic and Non-Thrombotic Disorders. Cambridge, United Kingdom: Cambridge University Press; 2002:104-112.
31. Arber S, Barbayannis FA, Hanser H, et al. Regulation of actin dynamics through phosphorylation of cofilin by LIM-kinase. Nature. 1998;393:805-809.
32. Yang N, Higuchi O, Ohashi K, et al. Cofilin phosphorylation by LIM-kinase 1 and its role in Rac-mediated actin reorganization. Nature. 1998;393:809-812.
33. Edwards DC, Sanders LC, Bokoch GM, Gill GN. Activation of LIM-kinase by Pak1 couples Rac/Cdc42 GTPase signalling to actin cytoskeletal dynamics. Nat Cell Biol. 1999;1:253-259.
34. Azim AC, Barkalow K, Chou J, Hartwig JH. Activation of the small GTPases, rac and cdc42, after ligation of the platelet PAR-1 receptor. Blood. 2000;95:959-964.
35. Vidal C, Geny B, Melle J, Jandrot-Perrus M, Fontenay-Roupie M. Cdc42/Rac1-dependent activation of the p21-activated kinase (PAK) regulates human platelet lamellipodia spreading: implication of the cortical-actin binding protein cortactin. Blood. 2002;100:4462-4469.
36. Fritsche J, Reber BF, Schindelholz B, Bandtlow CE. Differential cytoskeletal changes during growth cone collapse in response to hSema III and thrombin. Mol Cell Neurosci. 1999;14:398-418.
37. Gu Y, Ihara Y. Evidence that collapsin response mediator protein-2 is involved in the dynamics of

microtubules. J Biol Chem. 2000;275:17917-17920.

38. Schwarz UR, Walter U, Eigenthaler M. Taming platelets with cyclic nucleotides. Biochem Pharmacol. 2001;62:1153-1161.
39. Gabbeta J, Yang X, Kowalska MA, Sun L, Dhanasekaran N, Rao AK. Platelet signal transduction defect with Gα subunit dysfunction and diminished $G\alpha_q$ in a patient with abnormal platelet responses. Proc Natl Acad Sci U S A. 1997;94:8750-8755.
40. Freedman JE, Loscalzo J, Barnard MR, Alpert C, Keaney JF, Michelson AD. Nitric oxide released from activated platelets inhibits platelet recruitment. J Clin Invest. 1997;100:350-356.
41. Hartwig JH, Bokoch GM, Carpenter CL, et al. Thrombin receptor ligation and activated Rac uncap actin filament barbed ends through phosphoinositide synthesis in permeabilized human platelets. Cell. 1995;82:643-653.
42. Burridge K, Wennerberg K. Rho and Rac take center stage. Cell. 2004;116:167-179.
43. Takenawa T, Miki H. WASP and WAVE family proteins: key molecules for rapid rearrangement of cortical actin filaments and cell movement. J Cell Sci. 2001;114:1801-1809.
44. Oda A, Miki H, Wada I, et al. WAVE/Scars in platelets. Blood. Prepublished on August 3, 2004, as DOI 10.1182/blood-2003-04-1319. (Now available as Blood. 2005;105:3141-3148.
45. Kashiwagi H, Shiraga M, Kato H, et al. Expression and subcellular localization of WAVE isoforms in the megakaryocyte/platelet lineage. J Thromb Haemost.2005;3:361-368.
46. Jin Z, Strittmatter SM. Rac1 mediates collapsin-1-induced growth cone collapse. J Neurosci. 1997;17:6256-6263.
47. Kuhn TB, Brown MD, Wilcox CL, Raper JA, Bamburg JR. Myelin and collapsin-1 induce motor neuron growth cone collapse through different pathways: inhibition of collapse by opposing mutants of rac1. J Neurosci. 1999;19:1965-1975.
48. Aizawa H, Wakatsuki S, Ishii A, et al. Phosphorylation of cofilin by LIM-kinase is necessary for semaphorin 3A-induced growth cone collapse. Nat Neurosci. 2001;4:367-373.
49. Hu H, Marton TF, Goodman CS. Plexin B mediates axon guidance in Drosophila by simultaneously inhibiting active Rac and enhancing RhoA signaling. Neuron. 2001;32:39-51.
50. Vikis HG, Li W, He Z, Guan KL. The semaphorin receptor plexin-B1 specifically interacts with active Rac in a ligand-dependent manner. Proc Natl Acad Sci U S A. 2000;97:12457-12462.
51. Driessens MH, Hu H, Nobes CD, et al. Plexin-B semaphorin receptors interact directly with active Rac and regulate the actin cytoskeleton by activating Rho. Curr Biol. 2001;11:339-344.
52. Turner LJ, Nicholls S, Hall A. The activity of the plexin-A1 receptor is regulated by Rac. J Biol Chem. 2004;279:33199-33205.
53. Zanata SM, Hovatta I, Rohm B, Puschel AW. Antagonistic effects of Rnd1 and RhoD GTPases regulate receptor activity in semaphorin 3A-induced cytoskeletal collapse. J Neurosci. 2002;22:471-477.
54. Peerschke EI. Observations on the effects of cytochalasin B and cytochalasin D on ADP- and chymotrypsin-treated platelets. Proc Soc Exp Biol Med. 1984;175:109-115.
55. Lefebvre P, White JG, Krumwiede MD, Cohen I. Role of actin in platelet function. Eur J Cell Biol. 1993;62:194-204.
56. Torti M, Festetics ET, Bertoni A, Sinigaglia F, Balduini C. Agonist-induced actin polymerization is required for the irreversibility of platelet aggregation. Thromb Haemost. 1996;76:444-449.
57. Bennett JS, Zigmond S, Vilaire G, Cunningham ME, Bednar B. The platelet cytoskeleton regulates the affinity of the integrin $\alpha_{IIb}\beta_3$ for fibrinogen. J Biol Chem. 1999;274:25301-25307.
58. Natarajan P, May JA, Sanderson HM, Zabe M, Spangenberg P, Heptinstall S. Effects of cytochalasin H, a potent inhibitor of cytoskeletal reorganisation, on platelet function. Platelets. 2000;11:467-476.
59. Hato T, Pampori N, Shattil SJ. Complementary roles for receptor clustering and conformational change in the adhesive and signaling functions of integrin $\alpha_{IIb}\beta_3$. J Cell Biol. 1998;141:1685-1695.
60. Tadokoro S, Shattil SJ, Eto K, et al. Talin binding to integrin β tails: a final common step in integrin activation. Science. 2003;302:103-106.
61. Calderwood DA. Integrin activation. J Cell Sci. 2004;117:657-666.
62. Brown NH, Gregory SL, Rickoll WL, et al. Talin is essential for integrin function in Drosophila. Dev Cell. 2002;3:569-579.
63. Jiang G, Giannone G, Critchley DR, Fukumoto E, Sheetz MP. Two-piconewton slip bond between fibronectin and the cytoskeleton depends on talin. Nature. 2003;424:334-337.

Journal of Thrombosis and Haemostasis, 3: 1–8 DOI: 10.1111/j.1538-7836.2005.01534.x

ORIGINAL ARTICLE

Association of the antagonism of von Willebrand factor but not fibrinogen by platelet $\alpha_{IIb}\beta_3$ antagonists with prolongation of bleeding time

T. AOKI,* Y. TOMIYAMA,† S. HONDA,† K. MIHARA,* T. YAMANAKA,‡ M. OKUBO,‡ A. MORIGUCHI* and S. MUTOH*

**Medicinal Biology, Research Laboratories, Fujisawa Pharmaceutical Co., Ltd, Kashima, Yodogawa-ku, Osaka, Japan; †Department of Internal Medicine and Molecular Science, Graduate School of Medicine B5, Osaka University, Yamadaoka, Suita, Osaka, Japan; and ‡Medicinal Chemistry Research Laboratories, Fujisawa Pharmaceutical Co., Ltd, Kashima, Yodogawa-ku, Osaka, Japan*

To cite this article: Aoki T, Tomiyama Y, Honda S, Mihara K, Yamanaka T, Okubo M, Moriguchi A, Mutoh S. Association of the antagonism of von Willebrand factor but not fibrinogen by platelet $\alpha_{IIb}\beta_3$ antagonists with prolongation of bleeding time. *J Thromb Haemost* 2005; DOI: 10.1111/j.1538-7836.2005.01534.x.

Summary. *Background:* The $\alpha_{IIb}\beta_3$ antagonists inhibit platelet aggregation and are used as antithrombotic agents for cardiothrombotic disease. The present study investigates the correlation of inhibition of fibrinogen and von Willebrand factor (VWF) binding by $\alpha_{IIb}\beta_3$ antagonists with the inhibition of platelet aggregation and prolongation of bleeding time (BT). *Methods:* Inhibition of fibrinogen and VWF binding were assessed in a purified $\alpha_{IIb}\beta_3$-binding assay. As an *in vitro* cell-based assay, platelet aggregation and VWF-mediated adhesion studies were performed using human platelets. *In vivo* effects on BT were measured using a template device in dogs at the same time as an *ex vivo* aggregation study was performed. *Results: In vitro* studies demonstrated that the antiaggregatory effects of $\alpha_{IIb}\beta_3$ antagonists correlate with their inhibition of fibrinogen binding, but not VWF. Interestingly, the effects of $\alpha_{IIb}\beta_3$ antagonists on BT could be differentiated from the inhibition of platelet aggregation. Furthermore, this differentiation was strongly correlated with the different inhibitory potencies between fibrinogen and VWF binding, as well as that between VWF-mediated adhesion and aggregation. *Conclusions:* Our study provides novel evidence showing that the inhibitory effect of $\alpha_{IIb}\beta_3$ antagonists on VWF, but not fibrinogen binding, correlates with their ability to prolong BT.

Keywords: bleeding, fibrinogen, platelet $\alpha_{IIb}\beta_3$ antagonists, von Willebrand factor.

Correspondence: Toshiaki Aoki, Exploratory Research Laboratories, Fujisawa Pharmaceutical Co., Ltd, 2-3, Tokodai, 5-Chome, Tsukuba 300-2698, Japan.
Tel.: +81 29 847 8611; fax: +81 29 847 1536; e-mail: toshiaki_aoki@po.fujisawa.co.jp

Received 15 September 2005, accepted 28 April 2005

Introduction

Platelet aggregation and adhesion are key mechanisms for normal hemostasis and limiting blood loss from injured tissue [1,2]. $\alpha_{IIb}\beta_3$, the major integrin on the surface of the platelet membrane, is a physiologic receptor for fibrinogen and von Willebrand factor (VWF). The binding of these two ligands plays a crucial role in platelet aggregation and adhesion, in the initial process of thrombus formation. Antagonism of $\alpha_{IIb}\beta_3$ is an attractive strategy for antiplatelet therapy and achieves complete inhibition of aggregation [3,4]. Several $\alpha_{IIb}\beta_3$ antagonists have been used as antithrombotic drugs, and have demonstrated favorable efficacy in reducing the incidence of ischemic events in unstable angina and in preventing vascular events after percutaneous transluminal coronary angioplasty (PTCA) [5–7], although they appeared to increase the risk of bleeding [8,9]. Thus, careful management and monitoring of patients, such as weight adjustment of heparin dose and assessment of hemostatic markers [10–11], is required to avoid bleeding complications. Mechanistic studies on the hemorrhagic properties of $\alpha_{IIb}\beta_3$ antagonists would provide more detailed information about controlling bleeding complications.

Current mechanistic studies on platelet-thrombus formation under flow conditions suggest that the $\alpha_{IIb}\beta_3$ ligands, VWF and fibrinogen, play different functions in the process of thrombus formation. In the initial process of hemostasis, VWF binding to $\alpha_{IIb}\beta_3$ is a key step for formation of platelet adhesion, causing the initial surface coverage of injured vascular lumen. In contrast, fibrinogen binding plays a major role in the later phase of thrombus formation on the covered surface by recruiting platelet aggregates [12–14], and leads to formation of a mature thrombus to plug the injured vessels. Therefore, we hypothesized, if inhibition of the VWF-dependent surface coverage by platelets is the critical hemorrhagic determinant for $\alpha_{IIb}\beta_3$ antagonists, rather than the later fibrinogen-dominant phase, $\alpha_{IIb}\beta_3$ antagonists with minimal inhibition of VWF

binding should show reduced tendency for prolonged bleeding time (BT) but retain potent antiaggregation effects.

In this study, we assessed the inhibitory effects of synthetic $\alpha_{IIb}\beta_3$ antagonists on VWF and fibrinogen binding and examined their association with *ex vivo* inhibition of platelet aggregation and an *in vivo* hemorrhagic effect, prolongation of BT.

Materials and methods

Materials

FK419 [15], FK633 [16], FR184764, FR233229, FR231643, lamifiban [17], xemilofiban [18], and tirofiban [19] (Fig. 1) were synthesized in Fujisawa Pharmaceutical Co., Ltd (Osaka, Japan), with purity >98% by HPLC and mass spectrum analysis. All antagonists were dissolved in isotonic sodium chloride solution or buffer prior to use.

Proteins and antibodies

Fibrinogen and VWF were purchased from American Diagnostica Inc. (Stamford, CT, USA). Purified human $\alpha_{IIb}\beta_3$ was purchased from Enzyme Research Laboratories Inc. (IN, USA). Anti-$\alpha_{IIb}\beta_3$ (PT25-2) was purchased from Takara, (Japan). HPR-F(ab')$_2$ fragments of goat antimouse IgG (H + L) antibody was purchased from Zymed Laboratories Inc. San Francisco, (CA, USA) . Bovine serum albumin (BSA) was purchased from Nakarai (Japan).

Inhibition assay for the interaction of purified $\alpha_{IIb}\beta_3$ with fibrinogen and von Willebrand factor

Fibrinogen (1 μg per well) was immobilized on a 96-well microtiter plate overnight at 4 °C. The residual exposed plastic was blocked with 1% BSA. After the plate was washed twice with buffer, 50 μL of purified $\alpha_{IIb}\beta_3$ at 20 μg mL^{-1} in the presence or absence of 50 μL of drug were added to each well and incubated for 3 h at room temperature. Bound $\alpha_{IIb}\beta_3$ was measured by ELISA by using primary (antihuman $\alpha_{IIb}\beta_3$) and secondary (goat antimouse IgG coupled to HPR) antibodies. In the case of VWF-binding assay, $\alpha_{IIb}\beta_3$ was immobilized on the plate. VWF was added and binding was measured by ELISA. IC_{50} values were calculated by using the curve fitting and statistics software, PRISM version 4, and are expressed as the mean ± SEM of five experiments. All experiments were performed with the same lot of the proteins. $\alpha_{IIb}\beta_3$ antagonists were compared under the same assay conditions. We also measured K_d values for fibrinogen and VWF binding in our assay formats. The K_d values (Fg: K_d = 87 nM, VWF: K_d = 11 nM) were comparable with those reported in the literature [20,21].

Platelet adhesion to von Willebrand factor coated plate

Venous blood from healthy male volunteers was collected onto sodium citrate. Platelet-rich plasma (PRP) was prepared by rapid centrifugation of whole blood. Platelets were washed with modified HEPES-Tyrode's buffer containing 1 μM PGE_1. After washing, platelets were suspended in modified HEPES-Tyrode's buffer containing 1.0 mM $CaCl_2$ without PGE_1, and platelet count was adjusted. Adhesion assay protocol was performed as described previously [22]. Briefly, 96-well microtiter plates were coated with 1 μg per well of VWF. The plates were then blocked with 1% BSA. After washing the plates with buffer, ADP-activated washed platelets were added to each well in presence of drugs or buffer and incubated for 30 min at 37 °C. The plates were then washed three times with buffer. The number of adhered cells was determined by the acid

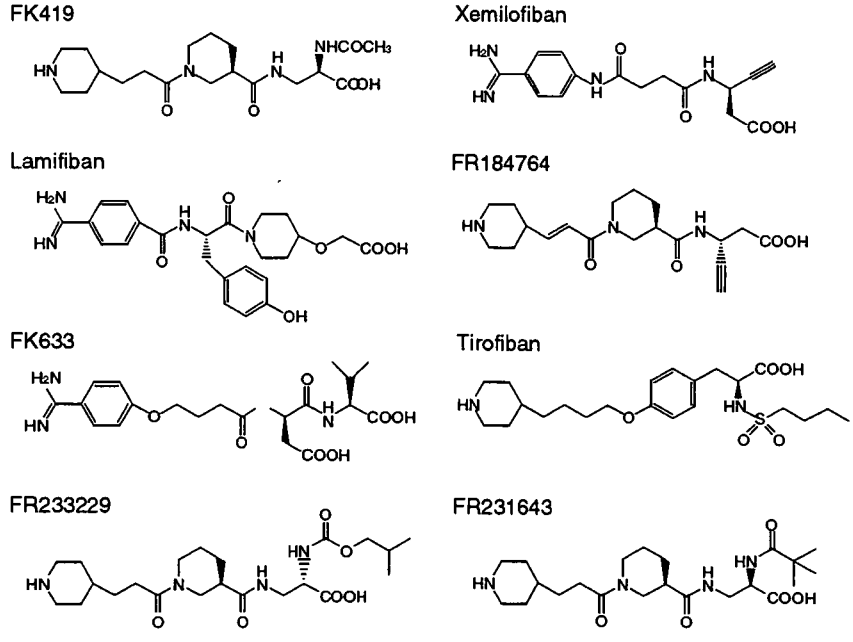

Fig. 1. Chemical structures of synthetic $\alpha_{IIb}\beta_3$ antagonists.

phosphatase activity of cells at 410 nm using a microplate reader.

Platelet aggregation study

Platelet aggregation assays were performed using NBS HEMA TRACER 801, an eight-channel aggregometer (Nikobioscience, Tokyo, Japan). Light transmittance of PPP was calibrated as 100%. PRP was incubated for 2 min in the aggregometer at 37 °C. ADP (2.5 μM for humans and 20–40 μM for dogs) was added as an agonist at which full response of platelet aggregation was obtained, and the change in light transmittance was monitored by a PL500 recorder (Yokogawa, Tokyo, Japan). Percent inhibition of aggregation in the drug-treated samples was calculated by comparison with the aggregation in the absence of drug or in the pretreatment period.

Measurement of template bleeding time

All experiments were carried out in accordance with the guidelines provided by the Ethical Committee of Fujisawa Pharmaceutical Co., Ltd. Beagle dogs (Kashou Co., Ltd or Japan Laboratory Animals Co., Ltd, Tokyo, Japan) were anesthetized with sodium pentobarbital at 30 mg kg^{-1} intraperitoneally. $\alpha_{IIb}\beta_3$ antagonists were administered by a bolus injection (0.2 mL kg^{-1}), followed by continuous infusion (0.1 mL kg^{-1} h^{-1}) for 3 h, from a catheter inserted into the vein on the surface of the hind limb. Blood samples were taken six time-points from the cephalic vein for the platelet aggregation study and for measurement of plasma drug concentrations at 30-min intervals after dosing. At the same time as blood sample collection, BT was assessed with an automated spring-loaded device (Simplete R, Organon Teknika, Durham, NC, USA) designed to produce a standardized incision applied to the inner side of the upper jowl. Blood from the incision was blotted with Whatman No.2 filter paper every 30 s until all bleeding had stopped. In order to eliminate the experimental validity, we have excluded animals with the basal BT of > 5 or < 3 min. Our laboratory standard of basal BT was 3.9 ± 0.3 min. When bleeding did not stop within 30 min, BT was recorded as 30 min. Prolongation of BT was determined by comparison with the time in the pretreatment period.

Determination of plasma concentration of $\alpha_{IIb}\beta_3$ antagonists

Plasma samples were mixed with water, and purified by solid-phase extraction. The eluate was evaporated under a nitrogen stream, dissolved in water, and analyzed by LC-MS-MS. HPLC separation was achieved using a mobile phase consisting of formate buffer/acetonitrile/methanol with flow rate 0.2 mL min^{-1}. The lower limit of quantification was 10 ng mL^{-1} using 50 μL plasma, and intra-day precision measurements of the assay as indicated by coefficients of variation were $< 10\%$.

Calculation of mean plasma concentrations for 50% inhibition of platelet aggregation and for 2.5-fold prolongation of bleeding time

Data for inhibition of ADP-induced *ex vivo* platelet aggregation (Yi%) and prolongation of BT (Zi-fold) at all doses and time points were sorted in order of increasing plasma concentrations (Xi, ng mL^{-1}) of an antagonist. Mean concentrations for 50% inhibition of platelet aggregation and 2.5-fold prolongation of BT were calculated using curve fitting and statistics software, PRISM version 4. The values are expressed as mean ± SEM.

Results

Inhibition of fibrinogen and von Willebrand factor binding to purified $\alpha_{IIb}\beta_3$

Inhibitory effects of synthetic $\alpha_{IIb}\beta_3$ antagonists on fibrinogen and VWF binding were determined by ELISA assays of purified $\alpha_{IIb}\beta_3$. In this binding assay, all antagonists effectively inhibited both fibrinogen and VWF binding to purified $\alpha_{IIb}\beta_3$ in a concentration-dependent manner (Fig. 2). Interestingly, the rank orders of antagonists for the inhibition were different between fibrinogen and VWF binding (fibrinogen inhibition; tirofiban < FK419 = xemilofiban < FK633, VWF inhibition; tirofiban ≤ xemilofiban < FK419 = FK633). For instance, FK419 inhibited VWF binding with similar potency as FK633; however, its potency for fibrinogen was fourfold higher than FK633. Thus, FK419 is a relatively selective inhibitor of fibrinogen binding compared with FK633. To validate the relative selectivity of $\alpha_{IIb}\beta_3$ antagonists, we calculate ratios of IC_{50}s for fibrinogen to VWF binding as a selectivity index, VWF/Fg (Table 1). The results of this study suggest that the selectivity index varied for each $\alpha_{IIb}\beta_3$ antagonist.

Inhibition of human platelet aggregation and von Willebrand factor-mediated adhesion

To further assess the cell-based antagonism of $\alpha_{IIb}\beta_3$ antagonists against fibrinogen and VWF, we assessed their inhibitory effects of the antagonists on ADP-induced aggregation and adhesion onto immobilized VWF *in vitro*. As summarized in Table 2, all antagonists were effective in inhibiting ADP-induced platelet aggregation (AG1) with IC_{50} values ranging from 21 to 103 nM, with comparable potency to their inhibition of fibrinogen binding to purified $\alpha_{IIb}\beta_3$. Furthermore, in the platelet adhesion assay, they also effectively inhibited ADP-activated platelet adhesion to VWF-coated plates. However IC_{50} values for VWF-mediated adhesion (AD) were not parallel to that for aggregation. The $\alpha_{IIb}\beta_3$ antagonists, xemilofiban, lamfiban, and tirofiban, showed similar or greater potency for inhibiting VWF-mediated adhesion compared with their inhibitory effects on platelet aggregation, and had a lower ratio (AD/AG1). In other words, these antagonists had lower ratios of AD/AG1 than those of FK419 and FR233229. The

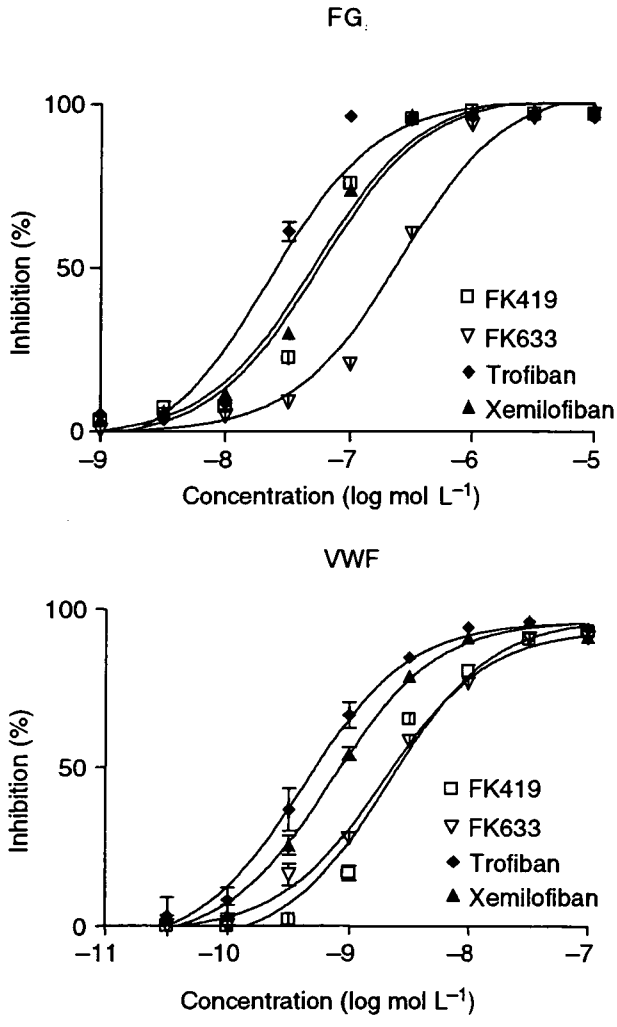

Fig. 2. Effects of synthetic $\alpha_{IIb}\beta_3$ antagonists, FK419, FK633, tirofiban, and lamifiban, on fibrinogen and von Willebrand factor binding to purified $\alpha_{IIb}\beta_3$ receptors. All experiments were performed by using the same protein preparation and assay plates. Data are presented as the mean ± SEM of five experiments.

Table 1 Inhibitory effects of $\alpha_{IIb}\beta_3$ antagonists for purified $\alpha_{IIb}\beta_3$-ligand binding

	Fibrinogen (Fg) IC_{50} (nM)	von Willebrand factor (VWF), IC_{50} (nM)	Ratio (VWF)/(Fg)
FK419	53 ± 2.7	3.2 ± 0.34	0.060
FK633	200 ± 14	2.8 ± 0.49	0.014
Xemilofiban	45 ± 0.2	0.87 ± 0.15	0.019
Lamifiban	20 ± 4.9	0.76 ± 0.06	0.038
Tirofiban	26 ± 0.2	0.73 ± 0.30	0.028
FR184764	34 ± 3.6	0.68 ± 0.14	0.020
FR233229	9.5 ± 0.6	0.47 ± 0.07	0.049
FR231643	24 ± 2.8	1.2 ± 1.3	0.050

results of cell-based studies suggest that each $\alpha_{IIb}\beta_3$ antagonists have different inhibitory effects between platelet aggregation and VWF-mediated platelet adhesion.

Table 2 Inhibitory effects of $\alpha_{IIb}\beta_3$ antagonists on platelet aggregation and von Willebrand factor-mediated adhesion

	ADP-induced aggregation (AG1), IC_{50} (nM)	VWF-mediated adhesion (AD) IC_{50} (nM)	Ratio (AD)/(AG1)
FK419	53 ± 8.3	219 ± 12	5.5
FK633	103 ± 5.3	190 ± 23	1.8
Xemilofiban	26 ± 7.8	29 ± 6.1	1.1
Lamifiban	45 ± 3.0	20 ± 1.6	0.44
Tirofiban	46 ± 7.6	6.7 ± 2.2	0.15
FR184764	43 ± 5.3	157 ± 10	3.7
FR233229	21 ± 1.1	92 ± 14	4.3
FR231643	37 ± 2.5	94 ± 6.2	2.5

Ex vivo *inhibition of ADP-induced platelet aggregation and template bleeding time*

The effects of dose escalation of $\alpha_{IIb}\beta_3$ antagonists, FK419, xemilofiban and lamifiban on ADP-induced *ex vivo* platelet aggregation and template BT are represented in Fig. 3. These antagonists effectively inhibited ADP-induced aggregation in a dose-dependent manner, with time-courses of inhibition that paralleled their pharmacokinetics (data not shown). In template BT measurements, all the antagonists prolonged BT in a dose dependent manner; however, their potency was not dependent on the inhibition of platelet aggregation. It is noteworthy that the i.v. administration of FK419 at doses of 200 + 70 μg kg^{-1} h^{-1} completely inhibited ADP-induced aggregation without any prolongation of BT. Even at 500 + 150 μg kg^{-1} h^{-1}, FK419 induced only modest prolongation of BT. In sharp contrast, xemilofiban and lamifiban markedly prolonged BT even at doses causing more than 70% (100 + 92 μg kg^{-1} h^{-1}) and 85% (200 + 70 μg kg^{-1} h^{-1}) inhibition of platelet aggregation, respectively.

To clarify the separation of the effects on BT and inhibition of aggregation, data points were plotted as a function of plasma concentrations attained during infusion of the four $\alpha_{IIb}\beta_3$ antagonists, FK419, FK633, xemilofiban, and lamifiban, at all time points and doses given (Fig. 4). In FK419-treated animals, plasma concentration-dependent inhibition of platelet aggregation and prolongation of BT were observed at different concentration ranges. Although FK419 completely inhibited platelet aggregation at plasma levels of ~300 ng mL^{-1}, it started to prolong BT at the levels over 700 ng mL^{-1}. However, in FK633, xemilofiban, or lamifiban-treated animals, prolongation of BT was observed in accordance with their inhibition of platelet aggregation. Table 3 summarizes the mean plasma concentrations of $\alpha_{IIb}\beta_3$ antagonists for inducing 50% inhibition of platelet aggregation (AG2), and 2.5-fold prolongation of BT compared with pretreatment value (BT). Antagonists such as xemilofiban and FK633 showed narrow differences between inhibition of aggregation and prolongation of BT, with BT/AG2 ratios of 2.7 and 2.2, respectively. On the contrary, FK419 and FR233229 had a wide separation of these

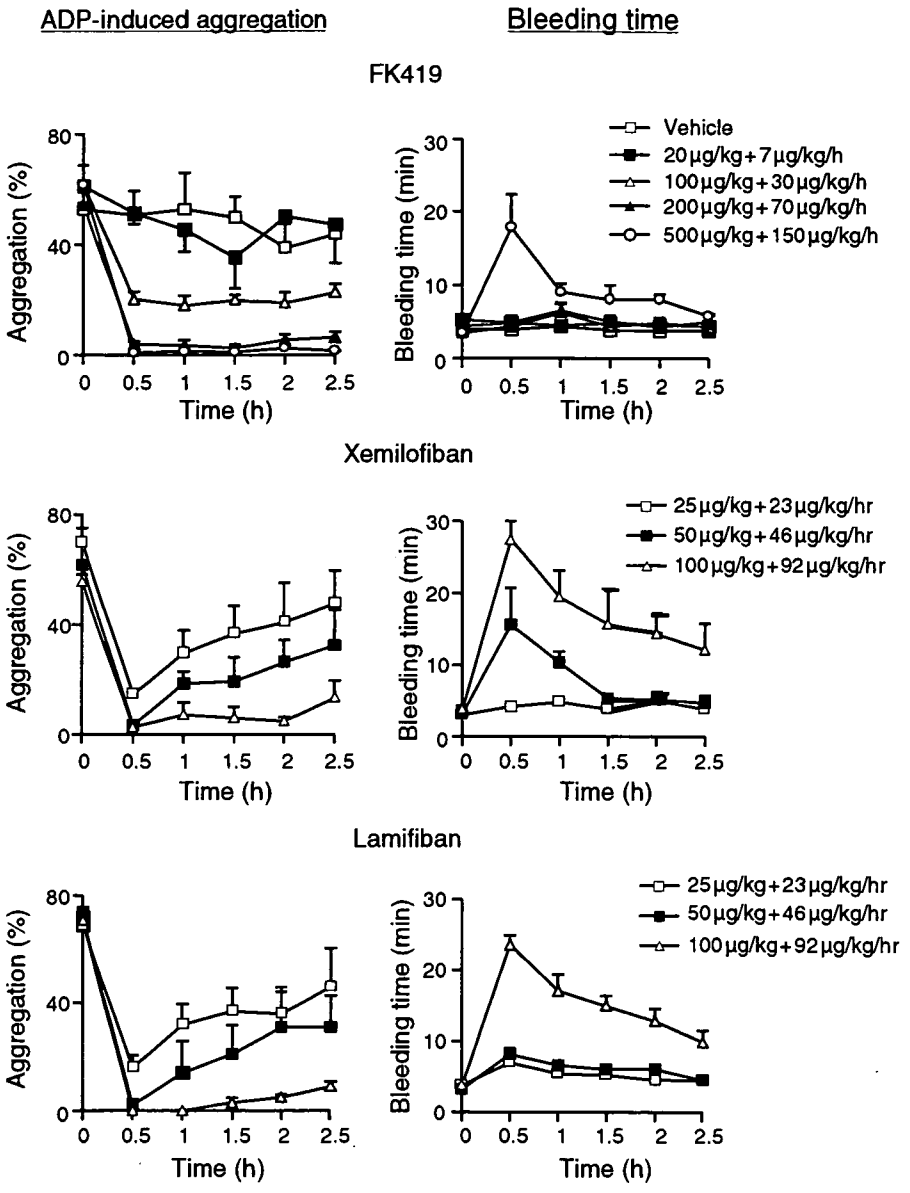

Fig. 3. Effects of synthetic $\alpha_{IIb}\beta_3$ antagonists on the platelet aggregation in response to ADP and template bleeding time during bolus plus continuous infusion in dogs. Data are presented as the mean ± SEM of four experiments.

parameters with a ratio of 17. These results suggest that the inhibitory effect of $\alpha_{IIb}\beta_3$ antagonists on platelet aggregation could be discriminated from their effect on BT.

Correlation between in vivo *BT/AG2 ratio and ligand selectivity, or* in vitro *AD/AG1*

To further investigate the mechanism of *in vivo* separation between inhibition of fibrinogen-mediated platelet aggregation and prolongation of BT (BT/AG2), we assessed the correlation between BT/AG2 and selectivity of the inhibition of ligand binding (VWF/Fg), or AD/AG1 obtained from *in vitro* platelet adhesion and aggregation studies. In Fig. 5a, BT/AG2 ratios for antagonists were plotted against ligand selectivity (VWF/Fg ratios). There was a good correlation between BT/AG2 ratios and VWF/Fg ($r = 0.81$, $n = 8$). These results suggest that the selectivity of antagonists for inhibition of two-ligand binding associate with separation between inhibition of aggregation and prolongation of BT. Moreover, as shown in Fig. 5b, there was also a strong correlation between BT/AG2 and AD/AG1 ratios ($r = 0.89$, $n = 8$). Together with the results of fibrinogen dependence of platelet aggregation, the present study strongly imply that inhibition of the interaction between $\alpha_{IIb}\beta_3$ and VWF is responsible for their hemorrhagic profile, prolongation of BT.

Discussion

The antagonism of platelet $\alpha_{IIb}\beta_3$ represents an attractive antithrombotic approach for the treatment of vaso-occlusive

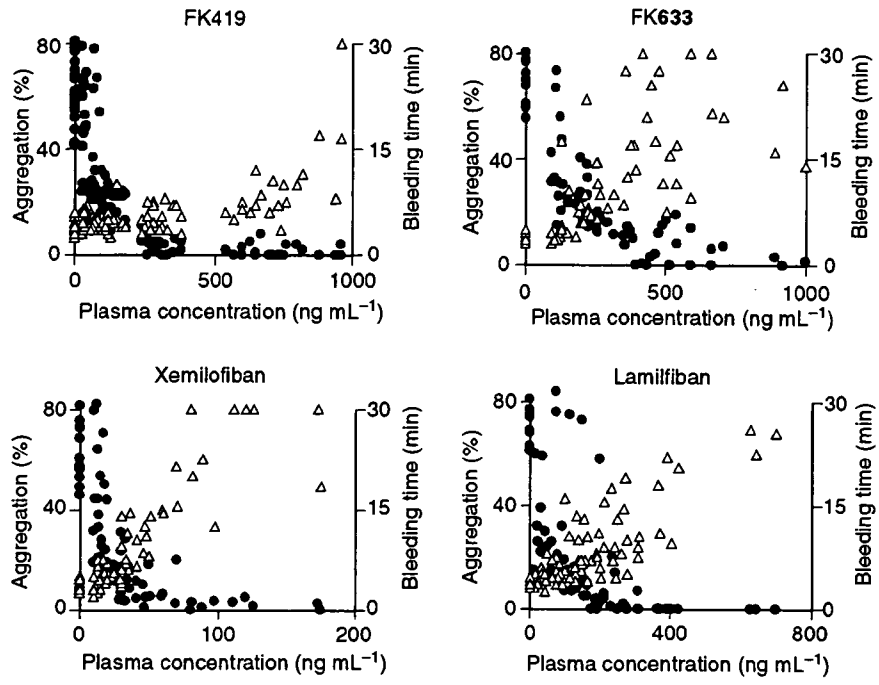

Fig. 4. Effects of synthetic $\alpha_{IIb}\beta_3$ antagonists on ADP-induced platelet aggregation (•) and template bleeding time (△) in dogs as a function of plasma concentrations of synthetic $\alpha_{IIb}\beta_3$ antagonists at all doses and time points.

Table 3 Inhibitory effects of antagonists on *ex vivo* platelet aggregation and bleeding time in dogs

	ADP-induced aggregation (AG2), IC_{50} (ng mL^{-1})	Bleeding time (BT), BT 2.5 (ng mL^{-1})	Ratio (BT)/(AG2)
FK419	46 ± 4.0	770 ± 20	17
FK633	108 ± 23	238 ± 16	2.2
Xemilofiban	16 ± 0.2	43 ± 1.6	2.7
Lamifiban	50 ± 5.4	212 ± 5.7	4.2
Tirofiban	57 ± 1.0	184 ± 5.8	3.2
FR184764	33 ± 1.0	260 ± 8.0	7.9
FR233229	2.8 ± 0.51	47 ± 3.0	17
FR231643	31 ± 3.0	244 ± 12	7.8

disorders. Intravenous $\alpha_{IIb}\beta_3$ antagonists such as abciximab, tirofiban, and integrelin, have been demonstrated to exert favorable efficacy in reducing the incidence of ischemic events in unstable angina as well as in preventing adverse events after PTCA [5–7]. However, a major concern of treatment with $\alpha_{IIb}\beta_3$ antagonists is the risk of critical bleeding. Early clinical studies with $\alpha_{IIb}\beta_3$ antagonists found substantial increases in the rate of major bleeding events and requirements for transfusion [8]. Therapeutic doses of these antagonists in unstable angina patients increase bleeding complications as well as BT by six to eightfold over baseline, when platelet aggregation is inhibited by > 80% [23]. Careful management and monitoring of patients are required to avoid bleeding

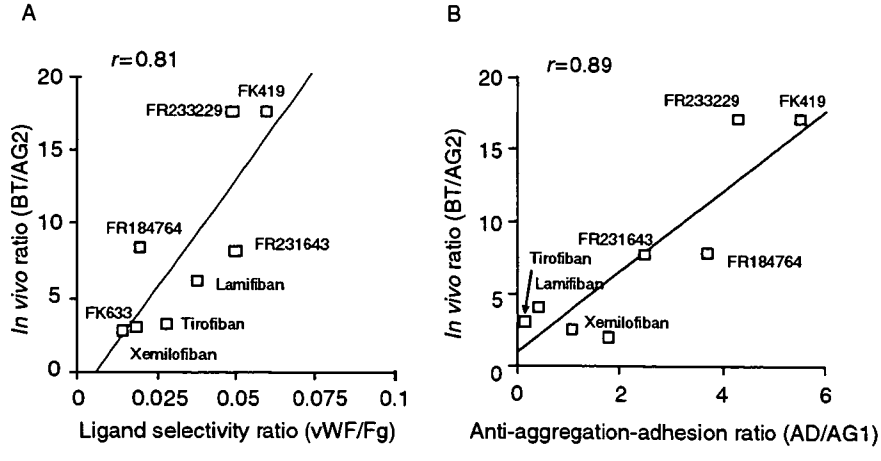

Fig. 5. Association of ligand selectivity or antiaggregation-adhesion effects of synthetic $\alpha_{IIb}\beta_3$ antagonists with the hemorrhagic profile. (A) Comparison of *in vitro* ligand selectivity (VWF/Fg) with *in vivo* safe separation between inhibition of platelet aggregation and prolongation of bleeding time (BT/AG2). (B) Comparison of *in vitro* antiaggregation–adhesion effects (AD/AG1) with *in vivo* safe separation between inhibition of platelet aggregation and prolongation of bleeding time (BT/AG2).

complications, including weight-adjustment of heparin dose and assessment of hemostatic markers.

In the present *in vivo* and *ex vivo* studies, we have demonstrated the prolongation of BT caused by $\alpha_{IIb}\beta_3$ antagonists can be dissociated from their inhibition of *ex vivo* platelet aggregation. $\alpha_{IIb}\beta_3$ antagonists such as FK419 and FR233229 did not markedly prolong BT even though they completely inhibited platelet aggregation (high BT/AG2 ratios). In contrast, other antagonists such as xemilofiban and lamifiban showed poor dissociation between these two effects (low BT/AG2 ratios). This discrepancy cannot be explained by pharmacokinetic differences (e.g. rapid decline of plasma concentration of antagonists might underestimate the ability to prolong BT during measurement period). For example, FK419 showed less tendency to promote bleeding even with a slower decline in plasma concentration, compared with xemilofiban and lamifiban, which showed a relatively rapid decline. These results suggest that distinct mechanisms underlie the inhibition of platelet aggregation and prolongation of BT by $\alpha_{IIb}\beta_3$ antagonists.

In terms of the inhibitory effect of $\alpha_{IIb}\beta_3$ antagonists on platelet aggregation, it is well documented that fibrinogen binding to $\alpha_{IIb}\beta_3$ is crucial for platelet aggregation. It has been shown that genetic mutation of the fibrinogen γ-chain abolished platelet aggregation induced by similar condition as the present study [24]. Thus, we hypothesized that blockade of VWF binding by $\alpha_{IIb}\beta_3$ antagonist is responsible for the prolongation of BT. To prove this hypothesis, we have assessed the inhibitory effects of $\alpha_{IIb}\beta_3$ antagonists on fibrinogen and VWF binding using a purified receptor-binding assay. To classify the relative VWF selectivity of $\alpha_{IIb}\beta_3$ antagonists against fibrinogen, we determined the ratio of IC_{50} values for VWF to fibrinogen binding (VWF/Fg). When the parameter of *in vivo* bleeding tendency, BT/AG2, was plotted against VWF selectivity, VWF/Fg, there was a strong correlation between these parameters. We also assessed cell-based selectivity for VWF inhibition, and found that there was a strong correlation between bleeding tendency and VWF selectivity. Thus, inhibition of VWF binding by $\alpha_{IIb}\beta_3$ antagonists is responsible for their ability to prolong BT. This observation is in agreement with findings showing that $\alpha_{IIb}\beta_3$ ligands, fibrinogen, and VWF play functionally different roles in hemostasis. Under high flow conditions, VWF binding to $\alpha_{IIb}\beta_3$ is essential for the formation of the initial irreversible platelet adhesion. In contrast, fibrinogen binding to $\alpha_{IIb}\beta_3$ plays a key role in later thrombus growth and stabilization, including platelet aggregation [14,25]. As VWF binding is responsible for the initial arrest of bleeding, $\alpha_{IIb}\beta_3$ antagonists with stronger potency for VWF inhibition would be predicted to prolong BT.

One question raised by this study is why $\alpha_{IIb}\beta_3$ antagonists targeting the same receptor have different effects on VWF and fibrinogen binding. This difference could be explained by a difference in the binding sites within $\alpha_{IIb}\beta_3$ molecule. VWF contains an RGD motif as receptor recognition sequence, whereas fibrinogen binds to $\alpha_{IIb}\beta_3$ through a non-RGD motif in its γ-chain, indicating that the nature of binding is different between two ligands [26,27]. Several reports also indicate that $\alpha_{IIb}\beta_3$ contains two distinct and interacting ligand binding sites, and that small peptide ligands can binds to distinct sites and elicit different functional responses [28–30]. Therefore, the selectivity of $\alpha_{IIb}\beta_3$ antagonists for inhibition of fibrinogen vs. VWF binding probably originates from discrimination of binding sites within $\alpha_{IIb}\beta_3$. In fact, $\alpha_{IIb}\beta_3$ antagonists such as FK633 and xemilofiban, which have low VWF/Fg values, were modified from an RGD peptide structure, whereas FK419 and FR233229, which have high VWF/Fg values, more closely resemble the structure of the LDV peptide in the γ-chain of fibrinogen [31].

The prolongation of BT has been attributed to the effects on other RGD-dependent integrins, such as $\alpha_v\beta_3$ and $\alpha_5\beta_1$ [32], or to the calcium ion dependence of their antagonism [33]. However, all antagonists examined in the present study were selective for $\alpha_{IIb}\beta_3$ among RGD-dependent integrins, but still have different effects on BT. In terms of calcium ion dependence for inhibition of platelet aggregation, we also determined the relationship between prolongation of BT and inhibition of aggregation measured by heparinized platelets. However, no correlation was observed between the inhibition of aggregation and prolongation of BT (data not shown). Thus, integrin specificity and calcium dependence do not explain the dissociation of prolongation of BT and inhibition of platelet aggregation.

Debate still continues regarding the measurement of BT in man and its predictive value [34, 35]. However, platelets play a central role in the process of a hemostatic plug formation, as BT is prolonged in patients with platelet disorder or taking antiplatelet agents [36]. Thus, to ensure whether there are any differences of hemorrhagic property is between $\alpha_{IIb}\beta_3$ antagonists, further clinical evaluation and comparison of antagonists such as FK419 will elucidate its clinical relevance.

In conclusion, the effect of $\alpha_{IIb}\beta_3$ antagonists on BT could be discriminated from their inhibitory effect on platelet aggregation. The prolongation of BT for $\alpha_{IIb}\beta_3$ antagonists is dependent on the ability to inhibit VWF binding to $\alpha_{IIb}\beta_3$ Platelet cohesion mediated by the interaction of VWF with $\alpha_{IIb}\beta_3$ plays an important role in the process of a hemostatic plug formation at the site of the wound. Thus, our present study provides novel evidence showing that ligand selectivity of $\alpha_{IIb}\beta_3$ antagonists affects their hemorrhagic property, BT.

Acknowledgements

We thank Dr Jiro Seki and Dr Nobuya Matsuoka for critical reading of this manuscript. We also thank Dr Roymond Price for preparing this manuscript.

Disclosure of conflicts of interest

The authors declare that they have no conflicts of interest.

References

1 Weiss HJ. Platelet physiology and abnormalities of platelet function (first of two parts). *N Engl J Med* 1975; **293**: 531–41.

2 Weiss HJ. Platelet physiology and abnormalities of platelet function (second of two parts). *N Engl J Med* 1975; **293**: 580–8.

3 Pytele R, Pierschbacher MD, Ginsberg MH, Plow EF, Ruoslahti E. Platelet membrane glycoprotein IIb/IIIa: member of a family of Arg-Gly-Asp-specific adhesion receptors. *Science* 1986; **231**: 1559–62.

4 Phillips DR, Charo IF, Scarborough RM. GPIIb-IIIa: the responsive integrin. *Cell* 1991; **65**: 359–62.

5 The EPIC Investigators. Use of a monoclonal antibody directed against the platelet glycoprotein IIb/IIIa receptor in high-risk coronary angioplasty. The EPIC Investigation. *N Engl J Med* 1994; **330**: 956–61.

6 The RESTORE Investigators. Effects of platelet glycoprotein IIb/IIIa blockade with tirofiban on adverse cardiac events in patients with unstable angina or acute myocardial infarction undergoing coronary angioplasty. The RESTORE Investigators. Randomized Efficacy Study of Tirofiban for Outcomes and REstenosis. *Circulation* 1997; **96**: 1445–53.

7 The PURSUIT Trial Investigators. Inhibition of platelet glycoprotein IIb/IIIa with eptifibatide in patients with acute coronary syndromes. The PURSUIT Trial Investigators. Platelet Glycoprotein IIb/IIIa in Unstable Angina: Receptor Suppression Using Integrilin Therapy. *N Engl J Med* 1998; **339**: 436–43.

8 Aguirre FV, Topol EJ, Ferguson JJ, Anderson K, Blankenship JC, Heuser RR, Sigmon K, Taylor M, Gottlieb R, Hanovich G, Rosenberg M, Donohue TJ, Weisman HF, Califf RM, for the EPIC Investigators. Bleeding complications with the chimeric antibody to platelet glycoprotein IIb/IIIa integrin in patients undergoing percutaneous coronary intervention. EPIC Investigators. *Circulation* 1995; **91**: 2882–90.

9 Harrington RA, Armstrong PW, Graffagnino C, Van De Werf F, Kereiakes DJ, Sigmon KN, Card T, Joseph DM, Samuels R, Granett J, Chan R, Califf RM, Topol EJ. Dose-finding, safety, and tolerability study of an oral platelet glycoprotein IIb/IIIa inhibitor, lotrafiban, in patients with coronary or cerebral atherosclerotic disease. *Circulation* 2000; **102**: 728–35.

10 The EPILOG Investigators. Platelet glycoprotein IIb/IIIa receptor blockade and low-dose heparin during percutaneous coronary revascularization. The EPILOG Investigators. *N Engl J Med* 1997; **336**: 1689–96.

11 Blankenship JC. Bleeding complications of glycoprotein IIb–IIIa receptor inhibitors. *Am Heart J* 1999; **138**: 287–96.

12 Savage B, Saldivar E, Ruggeri ZM. Initiation of platelet adhesion by arrest onto fibrinogen or translocation on von Willebrand factor. *Cell* 1996; **84**: 289–97.

13 Ruggeri ZM. The role of von Willebrand factor and fibrinogen in the initiation of platelet adhesion to thrombogenic surfaces. *Thromb Haemost* 1995; **74**: 460–3.

14 Matsui H, Sugimoto M, Mizuno T, Tsuji S, Miyata S, Matsuda M, Yoshida A. Distinct and concerted functions of von Willebrand factor and fibrinogen in mural thrombus growth under high shear flow. *Blood* 2002; **100**: 3604–10.

15 Mihara K, Aoki T, Moriguchi A, Yamamoto H, Maeda M, Tojo N, Yamanaka T, Ohkubo M, Matsuoka N, Seki J, Mutoh S. Characterization of the anti-platelet actions of FK419, a novel non-peptide antagonist of platelet GPIIb/IIIa. *Drug Dev Res* 2005; **61**: 233–41.

16 Aoki T, Harada K, Seki J, Tanaka A, Takasugi H, Motoyama Y. FK633: a potent and selective platelet GPIIb/IIIa antagonist. *Cardiovasc Drug Rev* 1999; **17**: 147–59.

17 Dooley M, Goa KL. Lamifiban. *Drugs* 1999; **57**: 215–21.

18 Nicholson NS, Panzer-Knodle SG, Salyers AK, Taite BB, Szalony JA, Haas NF, King LW, Zablocki JA, Keller BT, Broschat K, Engleman VW, Herin M, Jacqmin P, Feigen LP. SC-54684A: an orally active inhibitor of platelet aggregation. *Circulation* 1995; **91**: 403–10.

19 Cook JJ, Bednar B, Lynch JJ, Gould RJ, Egbertson MS, Halczenko W, Duggan ME, Hartman GD, Lo M-W, Murphy GM, Deckelbaum LI, Sax FL, Barr E. Tirofiban (Aggrastate®). *Cardiovasc Drug Rev* 1999; **17**: 199–224.

20 Huber W, Hurst J, Schlatter D, Barner R, Hubscher J, Kouns WC, Steiner B. Determination of kinetic constants for the interaction between the platelet glycoprotein IIb–IIIa and fibrinogen by means of surface plasmon resonance. *Eur J Biochem* 1995; **227**: 647–56.

21 De Marco L, Mazzucato M, De Roia D, Casonato A, Federici AB, Girolami A, Ruggeri ZM. Distinct abnormalities in the interaction of purified types IIA and IIB von Willebrand factor with the two platelet binding sites, glycoprotein complexes Ib-IX and IIb–IIIa. *J Clin Invest* 1990; **86**: 785–92.

22 Aoki T, Cox D, Senzaki K, Seki J, Tanaka A, Takasugi H, Motoyama Y. The anti-platelet and anti-thrombotic effects of FK633, a peptide-mimetic GPIIB/IIIA antagonist. *Thromb Res* 1996; **81**: 439–50.

23 Théroux P, Kouz S, Roy L, Knudtson ML, Diodati JG, Marquis JF, Nasmith J, Fung AY, Boudreault JR, Delage F, Dupuis R, Kells C, Bokslag M, Steiner B, Rapold HJ. Platelet membrane receptor glycoprotein IIb/IIIa antagonism in unstable angina: The Canadian lamifiban study. *Circulation* 1996; **94**: 899–905.

24 Bennett JS. Platelet-fibrinogen interactions. *Ann N Y Acad Sci* 2001; **936**: 340–54.

25 Tsuji S, Sugimoto M, Miyata S, Kuwahara M, Kinoshita S, Yoshioka A. Real-time analysis of mural thrombus formation in various platelet aggregation disorders: distinct shear-dependent roles of platelet receptors and adhesive proteins under flow. *Blood* 1999; **94**: 968–75.

26 Farrell DH, Thiagarajan P, Chung DW, Davie EW. Role of fibrinogen alpha and gamma chain sites in platelet aggregation. *Proc Natl Acad Sci* 1992; **89**: 10729–32.

27 Ruoslahti E. RGD and other recognition sequences for integrins. *Annu Rev Cell Dev Biol* 1996; **12**: 697–715.

28 Rooney MM, Farrell DH, van Hemel BM, de Groot PG, Lord ST. The contribution of the three hypothesized integrin-binding sites in fibrinogen to platelet-mediated clot retraction. *Blood* 1998; **92**: 2374–81.

29 Hu DD, White CA, Panzer-Knodle S, Page JD, Nicholson N, Smith JW. A new model of dual interacting ligand binding sites on integrin alphaIIbbeta3. *J Biol Chem* 1999; **274**: 4633–9.

30 Cierniewski CS, Byzova T, Papierak M, Haas TA, Niewiarowska J, Zhang L, Cieslak M, Plow EF. Peptide ligands can bind to distinct sites in integrin alphaIIbbeta3 and elicit different functional responses. *J Biol Chem* 1999; **274**: 16923–32.

31 Hoekstra WJ, Beavers MP, Andrade-Gordon P, Evangelisto MF, Keane PM, Press JB, Tomko KA, Fan F, Kloczewiak M, Mayo KH, Durkin KA, Liotta DC. Design and evaluation of nonpeptide fibrinogen gamma-chain based GPIIb/IIIa antagonists. *J Med Chem* 1995; **38**: 1582–92.

32 Tschopp JF, Mazur C, Gould K, Connolly R, Pierschbacher MD. Inhibition of thrombosis by a selective fibrinogen receptor antagonist without effect on bleeding time. *Thromb Haemost* 1994; **72**: 119–24.

33 Collen D, Lu HR, Stassen JM, Vreys I, Yasuda T, Bunting S, Gold HK. Antithrombotic effects and bleeding time prolongation with synthetic platelet GPIIb/IIIa inhibitors in animal models of platelet-mediated thrombosis. *Thromb Haemost* 1994; **71**: 95–102.

34 De Caterina R, Lanza M, Manca G, Strata GB, Maffei S, Salvatore L. Bleeding time and bleeding: an analysis of the relationship of the bleeding time test with parameters of surgical bleeding. *Blood* 1994; **84**: 3363–70.

35 Lind SE. The bleeding time does not predict surgical bleeding. *Blood* 1991; **77**: 2547–52.

36 Burns ER, Lawrence C. Bleeding time. A guide to its diagnostric and clinical utility. *Arch Pathol Lab Med* 1989; **113**: 1219–24.

Journal of Thrombosis and Haemostasis, 3: 1–9 DOI: 10.1111/j.1538-7836.2005.01554.x

ORIGINAL ARTICLE

Impaired platelet function in a patient with $P2Y_{12}$ deficiency caused by a mutation in the translation initiation codon

M. SHIRAGA,* S. MIYATA,† H. KATO,* H. KASHIWAGI,* S. HONDA,* Y. KURATA,‡ Y. TOMIYAMA* and Y. KANAKURA*

**Department of Hematology and Oncology, Graduate School of Medicine C9, Osaka University, Osaka, Japan; †Division of Blood Transfusion Medicine, National Cardiovascular Center, Osaka, Japan; and ‡Department of Blood Transfusion, Osaka University Hospital, Osaka, Japan*

To cite this article: Shiraga M, Miyata S, Kato H, Kashiwagi H, Honda S, Kurata Y, Tomiyama Y, Kanakura Y. Impaired platelet function in a patient with $P2Y_{12}$ deficiency caused by a mutation in the translation initiation codon. *J Thromb Haemost* 2005; DOI: 10.1111/j.1538-7836.2005.01554.x.

Summary. In this study, we have identified a patient (OSP-1) with a congenital $P2Y_{12}$ deficiency showing a mild bleeding tendency from her childhood and examined the role of $P2Y_{12}$ in platelet function. At low concentrations of agonists OSP-1 platelets showed an impaired aggregation to several kinds of stimuli, whereas at high concentrations they showed a specifically impaired platelet aggregation to ADP. ADP normally induced platelet shape change and failed to inhibit PGE_1-stimulated cAMP accumulation in OSP-1 platelets. Molecular genetic analysis revealed that OSP-1 was a homozygous for a mutation in the translation initiation codon (ATG to AGG) in the *P2Y*$_{12}$ gene. Heterologous cell expression of wild-type or mutant $P2Y_{12}$ confirmed that the mutation was responsible for the deficiency in $P2Y_{12}$. OSP-1 platelets showed a markedly impaired platelet spreading onto immobilized fibrinogen. Real-time observations of thrombogenesis under a high shear rate (2000 s^{-1}) revealed that thrombi over collagen were small and loosely packed and most of the aggregates were unable to resist against high shear stress in OSP-1. Our data suggest that secretion of endogenous ADP and subsequent $P2Y_{12}$-mediated signaling are critical for platelet aggregation, platelet spreading, and as a consequence, for stabilization of thrombus.

Keywords: $\alpha_{IIb}\beta_3$, initiation codon, mutation, $P2Y_{12}$ deficiency, platelets, thrombogenesis.

Introduction

Platelets play a crucial role not only in a hemostatic plug formation, but also in a pathologic thrombus formation, particularly within atherosclerotic arteries subjected to high shear stress [1,2]. As an initial step in thrombogenesis, platelets adhere to exposed subendothelial matrices such as von Willebrand factor (VWF) and collagen, then become activated and aggregate to each other. These processes are primarily mediated by platelet surface glycoproteins such as GPIb-IX-V, $\alpha_2\beta_1$, GPVI, and $\alpha_{IIb}\beta_3$ (GPIIb-IIIa) [3,4]. In addition, several mediators such as ADP, thromboxane A_2, and thrombin cause further platelet activation and recruitment of circulating platelets to the injury sites through activation of $\alpha_{IIb}\beta_3$ and subsequent binding of VWF and fibrinogen.

Recent studies have demonstrated that the critical role for ADP in arterial thrombogenesis [5–7]. ADP is actively secreted from platelet dense granules on platelet activation and is passively released from damaged erythrocytes and endothelial cells. Platelets possess at least two major G protein-coupled ADP receptors that are largely responsible for platelet responses to ADP: $P2Y_1$ and $P2Y_{12}$ [6]. $P2Y_1$ is the G_q-coupled receptor responsible for mediating platelet shape change and reversible platelet aggregation through intracellular calcium mobilization [8,9], whereas $P2Y_{12}$ is the G_i-coupled receptor responsible for mediating inhibition of adenylyl cyclase and sustained platelet aggregation [10–12]. $P2Y_{12}$ is the therapeutic target of efficacious antithrombotic agents, such as ticlopidine, clopidogrel, and AR-C compounds [5,6], and its congenital deficiency results in a bleeding disorder [13,14]. The analyses of patients with $P2Y_{12}$ deficiency as well as $P2Y_{12}$-null mice would provide more precise information about the role of $P2Y_{12}$ in platelet function than those using $P2Y_{12}$ inhibitors. To date, four different families with a defect in the expression or the function of $P2Y_{12}$ have been characterized [10,13–16]. In this study, we have described a patient with the congenital $P2Y_{12}$ deficiency due to a homozygous mutation in the translation initiation codon and analyzed the role of $P2Y_{12}$ in platelet aggregation, platelet spreading onto immobilized fibrinogen, and thrombogenesis on a type I collagen-coated surface under a high shear rate. Our present data have demonstrated a crucial role of $P2Y_{12}$ in various platelet functions.

Correspondence: Yoshiaki Tomiyama, Department of Hematology and Oncology, Graduate School of Medicine C6, Osaka University, 2-2 Yamadaoka, Suita Osaka 565-0871, Japan.
Tel.: +81 6 6879 3732; fax: +81 6 6879 3739; e-mail: yoshi@hp-blood.med.osaka-u.ac.jp

Received 2 November 2004, accepted 7 June 2005

Materials and methods

Patient history

The proband (OSP-1) is a 67-year-old Japanese female with a lifelong history of easy bruising. She (OSP-1) was born from non-consanguineous parents who had no hemorrhagic diathesis. Although she showed massive bleeding during delivery of her son, she had no history of transfusions. Patient OSP-1 showed normal platelet count, normal coagulation tests (prothrombin time and activated partial thromboplastin time) and slightly elevated plasma fibrinogen (398 mg dL^{-1}). Ivy bleeding time of the patient was consistently prolonged (> 15 min). Clot retraction by MacFarlane's method was normal (50%; normal values 40%–70%). Her son never suffered from a bleeding tendency. Informed consent for analyzing their platelet function and molecular genetic abnormalities was obtained from OSP-1, her husband and their son.

Preparation of platelet-rich plasma and washed platelet suspension

Platelet-rich plasma (PRP) for aggregation studies was prepared by a centrifugation of whole blood anticoagulated with citrate at 250 *g* for 10 min and then the platelet count was adjusted at 300×10^6 mL^{-1} by platelet-poor plasma. Washed platelets were prepared as previously described [17]. In brief, 6 volumes of freshly drawn venous blood from the patient, her husband, son or healthy volunteers were mixed with 1 volume of acid–citrate–dextrose (ACD; National Institutes of Health Formula A, NIH, Bethesda, MD, USA) and centrifuged at 250 *g* for 10 min to obtain PRP. After incubation with 20 ng mL^{-1} prostaglandin E1 (PGE_1; Sigma-Aldrich, St Louis, MO, USA) for 15 min, the PRP was centrifuged at 750 *g* for 10 min, washed three times with 0.05 mol L^{-1} isotonic citrate buffer containing 20 ng mL^{-1} PGE_1 and resuspended in an appropriate buffer.

Platelet aggregometry

Platelet aggregation using PRP was monitored by a model PAM-6C platelet aggregometer (Mebanix, Tokyo, Japan) at 37 °C with a stirring rate of 1000 r.p.m. as previously described [18]. Protease-activated receptor 1-activating peptide (PAR1 TRAP, SFLLRNPNDKYEPF) and adenosine 3′,5′-diphosphate (A3P5P) were purchased from Sigma-Aldrich Corp. $P2Y_{12}$ antagonist, AR-C6993MX (2-propylthio-D-fluoromethylene adenosine 5-triphosphate) was a kind gift from AstraZeneca (Loughborough, UK).

Flow cytometry and measurement of intracellular cAMP

Flow cytometric analysis using various monoclonal antibodies (mAbs) specific for platelet membrane glycoproteins was performed as previously described [19].

For measuring intracellular cAMP levels, samples of 200 μL of washed platelets (60×10^6) in Walsh buffer (137 mM of NaCl, 2.7 mM of KCl, 1.0 mM of $MgCl_2$, 3.3 mM of NaH_2PO_4, 3.8 mM of HEPES, 0.1% of glucose, 0.1% of BSA, pH 7.4) were incubated with 1 μmol L^{-1} PGE_1 for 15 min, and then platelets were stimulated with ADP or epinephrine. After incubation for 15 min, total cellular cAMP levels were measured using the Biotrak cAMP enzyme immunoassay system from Amersham Pharmacia Biotech (Piscataway, NJ, USA).

Platelet adhesion assay

Adhesion study was performed as previously described [20]. In brief, non-treated polystyrene 10 cm dishes were coated with 100 μg mL^{-1} human fibrinogen in 5 mL of phosphate-buffered saline (PBS) at 4 °C overnight. After washing with PBS, dishes were blocked with PBS containing 1% of bovine serum albumin (BSA) for 90 min at 37 °C. Aliquots (1 mL) of washed platelets (25×10^6 mL^{-1}) were added to the fibrinogen-coated dishes and incubated at 37 °C. After incubation for 40 min, adherent platelets were fixed with 3.7% formaldehyde, permeabilized with 0.1% Triton X-100 and stained with TRITC-conjugated phalloidin. Platelet morphology and degrees of spreading were determined by fluorescence microscopy (Olympus, Tokyo, Japan).

Platelet thrombus formation under flow conditions

The real-time observation of mural thrombogenesis on a type I collagen-coated surface under a high shear rate (2000 s^{-1}) was performed as previously described [21]. In brief, type I collagen-coated glass coverslips were placed in a parallel plate flow chamber (rectangular type; flow path of 1.9-mm width, 31-mm length, and 0.1-mm height). The chamber was assembled and mounted on a microscope (BX60; Olympus, Tokyo, Japan) equipped with epifluorescent illumination (BX-FLA; Olympus) and a charge-coupled device (CCD) camera system (U-VPT-N; Olympus). Whole blood containing mepacrine-labeled platelets obtained from OSP-1 or control subjects was aspirated through the chamber by a syringe pump (Model CFV-3200, Nihon Kohden, Tokyo, Japan) at a constant flow rate of 0.285 mL min^{-1}, producing a wall shear rate of 2000 s^{-1} at 37 °C.

Amplification and analysis of platelet RNA

Total cellular RNA of platelets was isolated from 20 mL of whole blood, and $P2Y_1$ or $P2Y_{12}$ mRNA was specifically amplified by reverse transcription-polymerase chain reaction (RT-PCR), as previously described [22]. The following primers were constructed based on the published sequence of $P2Y_{12}$ cDNA and used for the first round PCR for $P2Y_{12}$ cDNA: Y12F1, 5′-GGCTGCAATAACTACTACTTACTGG-3′ [sense, nucleotide(nt) −74 to −50]; Y12R4, 5′-CAGGACAGTGTAGAGCAGTGG-3′ (antisense, nt 85 to 105) [10].

Allele-specific restriction enzyme analysis (ASRA)

Genomic DNA was isolated from mononuclear cells using SepaGene kit (Sanko Junyaku Co Ltd, Tokyo, Japan). Amplification of the region around the initiation codon of the $P2Y_{12}$ gene was performed by using primers BsrDI-GF, 5′-CTTTTGTTCTCTAGGTAACCAACAAGCAA-3′ (sense, the mismatched base is underlined), and Y12R4 (antisense described above) using 250 ng of DNA as a template. These primers can be found in GenBank accession no. AC024886.20 and the sense primer corresponds to 127558–127585. PCR products were then digested with restriction enzyme *BsrDI*. The resulting fragments were electrophoresed in a 6% polyacrylamide gel.

Construction of $P2Y_{12}$ expression vectors and cell transfection

The full-length cDNA of wild-type (WT) and mutant $P2Y_{12}$ was amplified by RT-PCR using primers Y12-*Hin*dIII-F, 5′-GAATTCAAGCTTCAAGAAATGCAAGCCGTCGACA-ACCTC-3′ (sense, nt −6 -21 for WT, *Eco*RI and *Hin*dIII sites introduced at the 5′ end were underlined) or Y12-*Hin*dIII-F2, 5′-GAATTCAAGCTTCAAGAAAGGCAAGCCGTCGAC-AACCTC-3′ (sense, nt −6 −21 for mutant), and Y12H-Not-R, 5′-TCTAGAGCGGCCGCTCAATGGTGATGGTGATGA-TGCATTGGAGTCTCTTCATT-3′ (antisense, nt 1012–1029, His × 6 were introduced before stop codon, *Not*I and *Xba*I sites introduced at the 5′ end were underlined). The amplified fragments were digested with *Hin*dIII and *Not*I, and the resulting 1059-bp fragments (nt −9 −1050) were extracted using QIAquick gel extraction kit (Qiagen, GmbH, Germany). These fragments were inserted into the pcDNA3 (Invitrogen, San Diego, CA, USA) digested with *Hin*dIII and *Not*I. The fragments inserted were characterized by sequence analysis to verify the absence of any other substitutions and the proper insertion of the PCR cartridge into the vector.

A total of 10 μg of WT or mutant $P2Y_{12}$ construct was transfected into human embryonic kidney 293 cells (HEK293 cells, 10^6 cells) using the calcium phosphate method as previously described [22]. Transfectants were lyzed by 1% Triton X-100 PBS containing protease inhibitors 2 days after transfection, and proteins were separated by 7.5% SDS-PAGE. After transferred onto a PVDF membrane, expressed proteins were detected by rabbit anti-His tag antibody.

Results

Platelet aggregation studies

We first examined the expression of platelet membrane glycoproteins in OSP-1 by flow cytometry. The patient's platelets (OSP-1 platelets) normally express GPIb-IX, $\alpha_{IIb}\beta_3$ (GPIIb-IIIa), $\alpha_2\beta_1$, and CD36 (data not shown). Fig. 1 shows platelet aggregation of PRP in response to various agonists. The aggregation of OSP-1 platelets induced by 20 μM of ADP was markedly impaired with only a small and transient

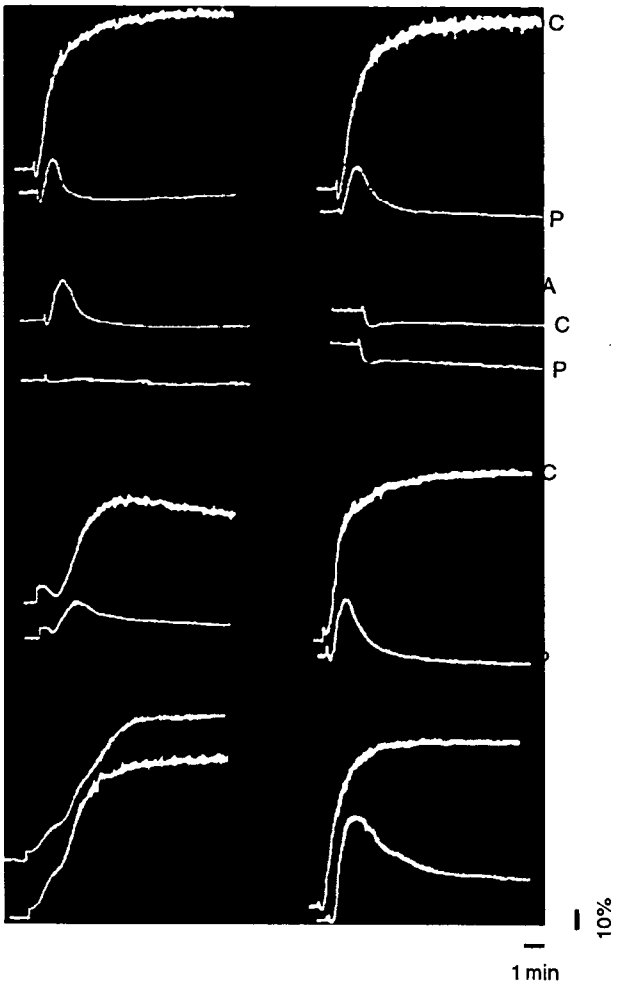

Fig. 1. Platelet aggregation induced by various agonists. Platelet aggregation was induced by various agonists in citrated PRP from patient OSP-1 (labeled 'P') or a control subject (labeled 'C'). Agonists used are (A) 20 μM of ADP, (B) 100 μM of ADP, (C) 20 μM of ADP in the presence of 1 μM of AR-C69931MX ('AR-C'), a specific $P2Y_{12}$-antagonist, or 1 mM of A3P5P ('A3P5P'), a specific $P2Y_1$-antagonist, (D) 20 μM of ADP in the presence of 5 mM of EDTA, (E) 0.5 μg mL^{-1} of collagen, (F) 0.63 μM of U46619, (G) 10 μM of epinephrine, and (H) 25 μM of PAR1-TRAP.

aggregation (Fig. 1A), and the aggregation was still impaired even at 100 μM of ADP (Fig. 1B). As compared with control platelets, the aggregation of OSP-1 platelets was also impaired with a transient aggregation in response to low concentrations of collagen (0.5 μg mL^{-1}, Fig. 1E), U46619 (0.63 μM, Fig. 1F), or PAR1 TRAP (25 μM, Fig. 1H). In response to 1.3 mg mL^{-1} ristocetin (not shown) or 10 μM of epinephrine (Fig. 1G), OSP-1 platelets aggregated normally. When OSP-1 platelets were stimulated with 20 μM of ADP in the presence of 5 mM of EDTA, the light transmission decreased equivalent to control platelets suggesting that OSP-1 platelets changed shape normally (Fig. 1D). We then examined effects of ADP receptor antagonists on the aggregation of OSP-1 platelets induced by 20 μM of ADP. A total of 1 mM of A3P5P, a specific $P2Y_1$ antagonist, abolished the residual response of OSP-1 platelets to ADP, whereas 1 μM of AR-C69931MX, a specific $P2Y_{12}$